Blockade of Smad4 in transformed keratinocytes containing a Ras oncogene leads to hyperactivation of the Ras-dependent Erk signalling pathway associated with progression to undifferentiated carcinomas

Maite Iglesias[1], Pilar Frontelo[1], Carlos Gamallo[2] and Miguel Quintanilla*[,1]

[1]*Instituto de Investigaciones Biomédicas Alberto Sols CSIC-UAM, Arturo Duperier 4, 28029-Madrid, Spain; [2]Hospital de la Princesa, Departamento de Anatomía Patológica, Facultad de Medicina, UAM, 28029-Madrid, Spain*

Smad4 functions as a transcription factor in TGF-β signalling. We have investigated the role of Smad4 in the TGF-β_1 cell responses of transformed PDV keratinocytes, which contain a Ras oncogene, and of non-tumorigenic MCA3D keratinocytes, by transfecting both cell lines with a dominant-negative Smad4 construct. Smad4 mediates TGF-β_1-induced up-regulation of p21[Cip1] and growth arrest in MCA3D cells. However, in PDV keratinocytes, Smad4 is only partially involved in TGF-β_1-induced growth inhibition, and does not mediate enhancement of p21[Cip1] levels by the growth factor. TGF-β_1 activates Ras/Erk signalling activity in both cell lines. PD098059, a specific inhibitor of MEK, diminishes TGF-β_1-induced p21[Cip1] levels in PDV but not in MCA3D cells, suggesting an involvement of Erk in up-regulation of p21[Cip1] by TGF-β_1 in PDV cells. PDV dominant-negative Smad4 cell transfectants, but not MCA3D transfectants, showed constitutive hyperactivation of the Ras/Erk signalling pathway, increased secretion of urokinase, higher motility properties, and a change to a fibroblastoid cell morphology associated *in vivo* with the transition from a well differentiated to a poorly differentiated tumour phenotype. Infection of MCA3D control and dominant negative Smad4 cell transfectants with retroviruses carrying a Ras oncogene led to enhanced p21[Cip1] and urokinase secreted levels, independently of TGF-β_1 stimulation, that were reduced by PD098059. These results suggest that Smad4 acts inhibiting Ras-dependent Erk signalling activity in Ras-transformed keratinocytes. Loss of Smad4 function in these cells results in hyperactivation of Erk signalling and progression to undifferentiated carcinomas. *Oncogene* (2000) **19**, 4134–4145.

Keywords: TGF-β_1; Smad4; Ras; Erk; urokinase; carcinoma

Introduction

Transforming growth factor-β (TGF-β) regulates cell proliferation, differentiation, motility, adhesion, and death in most tissues, including epithelia (Massagué, 1990; Lahio and Keski-Oja, 1992). During the last years the idea of a dual function of TGF-β in epithelial carcinogenesis has gained considerable support. TGF-β acts as a suppressor of tumour formation by virtue of its role in inhibiting proliferation of epithelial cells (Alexandrow and Moses, 1995; Massagué, 1998), but it also stimulates malignant progression at later stages of tumorigenesis by inducing an epithelial-mesenchymal transition associated with the development of a highly aggressive undifferentiated type of tumour (Caulin *et al.*, 1995; Cui *et al.*, 1996; Oft *et al.*, 1996, 1998; Frontelo *et al.*, 1998; Portella *et al.*, 1998).

Studies on the mouse skin carcinogenesis model and on mammary epithelial cells suggest a synergistic co-operation between oncogenic Ras and TGF-β_1 to stimulate malignant progression (Oft *et al.*, 1996; Akhurst and Balmain, 1999). The effects of the growth factor on carcinoma cell invasiveness and metastasis appear to be direct and require signalling through the type II receptor (Oft *et al.*, 1998; Portella *et al.*, 1998).

TGF-β signals through formation of heteromeric complexes between type I and type II serine/threonine kinase receptors. After activation, the signal transducing type I receptor binds and phosphorylates Smad2/Smad3 proteins that associate with Smad4 in the cytoplasm, and these complexes, then, translocate into the nucleus in which they activate transcription of specific genes (see Massagué, 1998; Zhang and Derynck, 1999; for reviews). TGF-β signalling components, such as type II receptors and Smad proteins, have been shown to be inactivated by mutation or deletion in human cancers (Massagué, 1998). Particularly, Smad4 (DPC4) was originally identified as a tumour suppressor gene frequently inactivated in pancreatic and colon carcinomas. Reconstitution of Smad4 in colon carcinoma defective cells leads to suppression of tumorigenicity (Schwarte-Waldhoff *et al.*, 1999)

Several reports point to a rapid and direct activation of the Ras-mitogen-activated protein (MAP) kinase signalling pathway associated with growth inhibition by TGF-β in epithelial cells (Hartsough *et al.*, 1996; reviewed in Hartsough and Mulder, 1997). The growth inhibitory response to TGF-β appears to be mediated by induction of cyclin-dependent kinase (cdk) inhibitors, such as p21[Cip1] and p15[INK4B] (Datto *et al.*, 1995; Hannon and Beach, 1994; Reynisdóttir *et al.*, 1995). The signalling pathways involved in these TGF-β-induced gene responses remain an open question (see Massagué, 1998). Thus, p21[Cip1] appears to be a downstream target gene regulated by Smad4 in carcinoma cells (Grau *et al.*, 1997; Hunt *et al.*, 1998), while it has been reported that Ras and the MAP kinase pathway are required for up-regulation of p21[Cip1] by TGF-β in intestinal epithelial cells and human keratinocytes, respectively (Yue *et al.*, 1998; Hu

et al., 1999). The same appears to occur for TGF-β-mediated induction of other genes, such as the 3TP-lux reporter construct, which contains a known TGF-β-inducible plasminogen activator inhibitor-1 (PAI-1) promoter (Grau et al., 1997; Mucsi et al., 1996; de Winter et al., 1997). This scenario has been complicated as several reports demonstrate a cross-talk between the Smad and Ras-MAP kinase signalling pathways (reviewed in Zhang and Derynck, 1999). Recently, Kretzschmar et al. (1999) found that oncogenic Ras, acting via MAP kinases, inhibits TGF-β-induced nuclear accumulation of Smad2 and Smad3. However, another report has shown that constitutively active MEK, or inhibitors for MEK, have no effect on Smad activity in human keratinocytes (Hu et al., 1999).

In this work, we have analysed the role of Smad4 in the TGF-β_1 responses of immortalized (MCA3D) and transformed (PDV) mouse epidermal keratinocytes by transfecting both cell lines with a C-terminal truncated, dominant-negative, Smad4 construct (Lagna et al., 1996). MCA3D cells are non-tumorigenic and exhibit normal Ras and p53 genes, while PDV are chemically transformed keratinocytes and produce low metastatic well differentiated squamous cell carcinomas upon injection in mice (Caulin et al., 1995; Frontelo et al., 1998). PDV cells contain a mutated H-Ras gene and express relatively low levels of activated Ras proteins (Quintanilla et al., 1991). They also have inactivated p53 loci (Burns et al., 1991). Both cell lines are growth-inhibited by TGF-β_1, but they respond differentially to chronic treatment with the growth factor. While MCA3D cells are induced to terminal differentiation and cell death in response to TGF-β_1, the growth factor stimulates cell motility and invasiveness in PDV cells, which undergo a reversible epithelial-mesenchymal conversion linked to progression toward a metastatic poorly differentiated tumour phenotype (Caulin et al., 1995; Frontelo et al., 1998). The invasive response of PDV and other carcinoma cells to TGF-β_1 is associated with enhanced expression/secretion of urokinase (uPA) and of its inhibitor PAI-1 (Farina et al., 1998; Santibáñez et al., 1999). uPA is a serine proteinase that converts the inactive plasminogen into the broad-spectrum active proteinase plasmin, which in turn degrades many proteins of the extracellular matrix and activates other matrix metalloproteinases (Andreasen et al., 1997).

We show that inhibiting Smad4 in Ras-transformed keratinocytes leads to hyperactivation of the Ras/Erk signalling pathway, increased secretion of uPA, and progression to a poorly differentiated tumour phenotype. On the other hand, a switch between the Smad and Erk signalling pathways, depending on the presence of oncogenic Ras, appears to occur in keratinocytes to mediate induction of p21^{Cip1} by TGF-β_1.

Results

Smad4 mediates growth inhibition in both MCA3D and PDV keratinocytes

MCA3D and PDV cell lines were transfected either with a full-length Smad4 cDNA or with a C-terminal truncated dominant-negative Smad4 (1–514) construct, together with the pcDNA3 neomycine resistant vector. Previously, the presence of Smad4 transcripts in both cell lines was demonstrated by RT–PCR (data not shown). After transfection with the normal full-length cDNA, no viable clones were obtained from MCA3D cells; while several clones could be selected up to the third passage, in which they died, in the case of PDV cells. These results suggest that overexpression of Smad4 induces cell death in keratinocytes, as reported for other epithelial cells (Atfi et al., 1997), although this hypothesis was not further investigated. Stable clones transfected with the dominant-negative Smad4 (1–514) construct were isolated from both MCA3D and PDV cell lines (designated as 3DdnS and PdnS, respectively). Clones transfected with the pcDNA3 vector alone were also obtained (designated as 3DC and PC) to be used as controls.

The activity of Smad signalling in the transfectants was analysed by measuring TGF-β_1-induced nuclear accumulation of Smad2/Smad3 in immunofluorescence experiments using a specific anti-Smad2,3 antibody (Figure 1). In exponentially growing MCA3D and PDV cells, untreated with TGF-β_1, anti-Smad2,3 staining was predominantly cytoplasmic concentrated at the perinuclear region, although about 18% of the cells showed Smad2/Smad3 accumulated in the nucleus (Figure 1a,b). This percentage of unstimulated cells with Smad2,3 localized into the nucleus was probably as consequence of TGF-β factors present in the serum or secreted by their own cells. In any case, on addition of TGF-β_1, about 90% of MCA3D cells showed anti-Smad2,3 staining concentrated into the nucleus. This response was rapid, with a maximum at 20 min, and lasted for about 1 h (Figure 1b). PDV cells responded partially to TGF-β_1-induced nuclear translocation of Smad2,3. Anti-Smad2,3 nuclear staining was limited to about 40% of the cells at 30 min of treatment (Figure 1a,b), indicating a constitutive inhibition of Smad signalling in these transformed keratinocytes, likely because of the presence of a Ras oncogene (Kretzschmar et al., 1999). 3DdnS and PdnS transfectants did not respond to TGF-β_1 for nuclear accumulation of Smad2,3 (see in Figure 1c the results obtained with 3DdnS18, PdnS7 and PdnS8; other clones, such as 3DdnS16, 3DdnS17 and PdnS5, behaved similarly), while nuclear translocation of Smad proteins was stimulated in control clones as in the corresponding parental cell lines (not shown). These results clearly indicated that the Smad transduction pathway was blocked in the dominant-negative Smad4 transfectants.

Although MCA3D cells are most sensitive than PDV for TGF-β_1-induced growth inhibition, both cell lines are growth-inhibited by concentrations of TGF-β_1 above 1 ng/ml (Haddow et al., 1991). As shown in Figure 2, TGF-β_1, at 10 ng/ml, inhibited the growth of 3DC and PC control cell clones after 48 h of treatment. All of the dominant-negative Smad4 transfectant clones showed resistance to growth inhibition, but, while it was drastically reduced in 3DdnS cells (Figure 2a), a significant inhibition of growth was still induced by TGF-β_1 in PdnS clones (Figure 2b), suggesting that other signalling pathways, in addition to Smad, could be involved in the antiproliferative response of transformed keratinocytes to TGF-β_1.
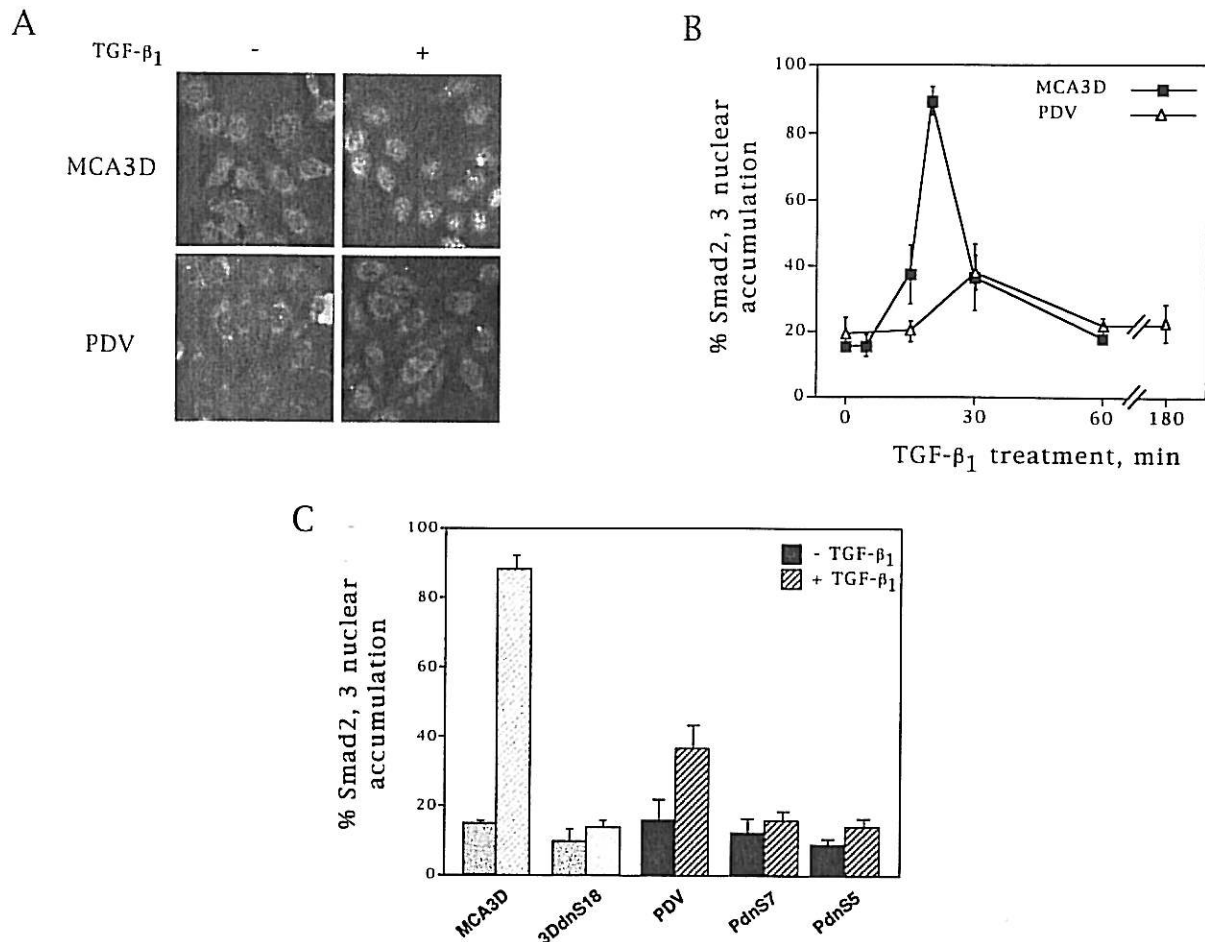
Figure 1 TGF-β_1-induced nuclear accumulation of Smad2/Smad3 in MCA3D and PDV cells, and in dominant-negative Smad4 transfectants. (a) Endogenous Smad2 and Smad3 were visualized by anti-Smad2,3 immunofluorescence staining in MCA3D and PDV cells untreated or treated with TGF-β_1 for 20 min and 30 min, respectively. (b) MCA3D and PDV cells were treated with TGF-β_1 for different time periods. Following immunofluorescence staining, the percentage of cells with Smad2,3 staining concentrated in the nucleus was calculated as described in Materials and methods. (c) Nuclear accumulation of Smad2,3 in response to TGF-β_1 in MCA3D, PDV and dominant-negative Smad4 transfectants. Treatments with the growth factor were of 20 min for MCA3D and 3DdnS18, and of 30 min for PDV, PdnS7 and PdnS5

We also analysed the activation by TGF-β_1 of 3TP-lux, a TGF-β-inducible reporter gene containing a PAI-1 promoter. Previous results indicated that TGF-β_1 induced a twofold activation of 3TP-lux in PDV cells after 24 h of treatment, while MCA3D cells were unable to respond to the growth factor for PAI-1 induction (Santibáñez et al., 1999). As shown in Figure 2c, TGF-β_1 activated 3TP-lux in the control PC2 clone (about twofold), while no significant activation of the reporter gene was found in PdnS transfectants. This result indicates that Smad4 is a key element in the TGF-β signal transduction cascade in transformed keratinocytes.

Smad4 mediates up-regulation of p21^{Cip1} by TGF-β_1 in MCA3D, but not in PDV cells in which the Erk signalling pathway is required

It has been demonstrated that TGF-β_1 induces the expression of the cdk inhibitor p21^{Cip1} in normal and transformed keratinocytes, and that induction of p21^{Cip1}, together with alterations in other cell cycle regulatory molecules, seems to be partially responsible of the growth-inhibitory effects of TGF-β_1 (Malliri et al., 1996). We studied the expression of

p21^{Cip1} in control and dominant-negative Smad4 cell transfectants by Western blot analysis of cell extracts obtained from synchronous exponentially growing cultures, untreated or treated with TGF-β_1 (Figure 3). No significant differences for induction of p21^{Cip1} in response to TGF-β_1 were observed when cells were cultured in the presence or absence of serum, although the basal protein levels of p21^{Cip1} (relative to the expression of β-actin, used as a protein loading marker) were higher when serum was present. Exposure to TGF-β_1 resulted in a fivefold induction of p21^{Cip1} protein expression in 3DC and PC control clones (Figure 3a–c). This response was blocked in 3DdnS transfectants (Figure 3a), while no differences for TGF-β_1 up-regulation of p21^{Cip1} were observed between control PC and dominant-negative PdnS transfectants (Figure 3b,c). Since the Erk MAP kinase signalling pathway has also been implicated in the regulation of p21^{Cip1} by TGF-β in epithelial cells (Yue et al., 1998; Hu et al., 1999), we studied the effects of PD098059, a specific inhibitor of MAP kinase kinase (MEK) (Simon et al., 1996), on p21^{Cip1} protein induction by TGF-β_1. PD098059, at a concentration of 50 μM (that is shown to inhibit efficiently Erk signalling activity in PDV cells, see
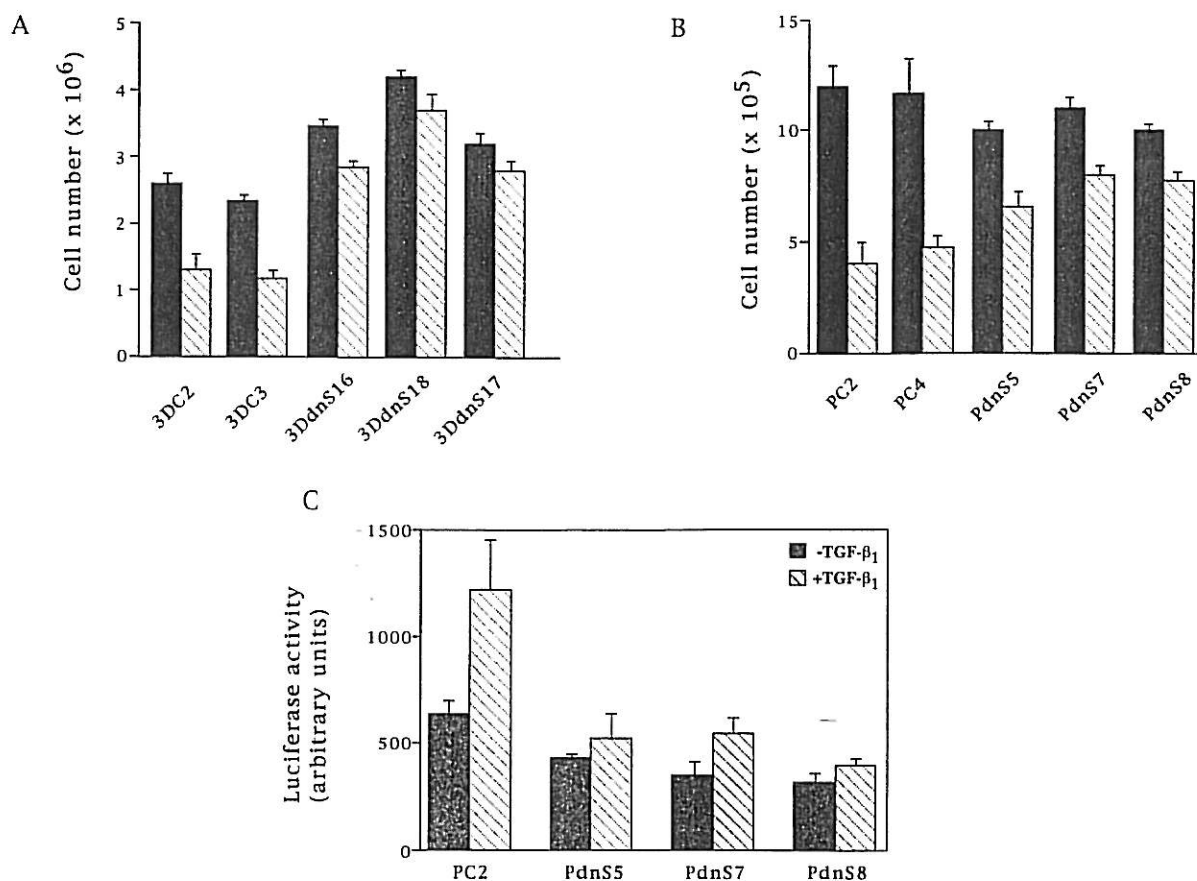
Figure 2 TGF-β_1-induced growth inhibition and transcriptional activation of the 3TP-lux reporter in the cell transfectants. (a, b) Cell growth inhibition assays in control (3DC, PC) and dominant-negative Smad4 (3DdnS, PdnS) transfectants. Synchronized cells, about 1×10^6 cells in (a) and 4.5×10^5 cells in (b), were seeded in 20-cm^2 culture dishes and grown in medium plus serum. TGF-β_1 treatment started on the following day. After 48 h, cells on TGF-β_1-treated (diagonally stripped bars) and untreated (black bars) dishes were counted. The figures represent the means ($\pm$s.d.) of quadruplicate incubations. (c) Induction of 3TP-lux by TGF-β_1 in PDV cell transfectants. Cells were transiently transfected with the 3TP-lux reporter plasmid and incubated without or with TGF-β_1 for 24 h. Luciferase activity in the cell lysates, corrected for transfection efficiency as indicated in Materials and methods, was plotted as the average (and s.d.) for duplicate determinations of two independent experiments

below), consistently reduced (by 35–50%) TGF-β_1-stimulated p21^{Cip1} expression in PC and PdnS clones, while it did not affect the enhancement of p21^{Cip1} by the growth factor in 3DC cells (Figure 3c). Altogether, these data indicated that Smad4 does not mediate regulation of p21^{Cip1} protein levels by TGF-β_1 in transformed PDV keratinocytes, and that this response appeared to require Erk MAP kinase signalling activity.

To study whether the expression of oncogenic Ras could explain the involvement of Erk in the modulation of p21^{Cip1} levels by TGF-β_1 in PDV cells, we infected 3DC and 3DdnS transfectants with retroviruses carrying an activated H-Ras gene, and analysed the levels of p21^{Cip1} in the absence and presence of TGF-β_1. Infection of the cells with the Harvey murine sarcoma virus (HMSV) produced a relatively high level of oncogenic Ras protein expression (see below), and resulted in a strong basal induction (4–7-fold) of p21^{Cip1} protein levels (Figure 3d,e). This increase was similar to that induced by TGF-β_1 in non-infected 3DC cells (Figure 3d), and occurred in both control and dominant-negative Smad4 transfectants. p21^{Cip1} protein levels in Ras-infected cells were significantly reduced by treatment with PD098059 (Figure 3e).

TGF-β_1 induces a rapid and transient activation of Ras and Erk in MCA3D and PDV keratinocytes

Therefore, we studied whether TGF-β_1 was able to activate the Ras/Erk signalling pathway in MCA3D and PDV keratinocytes. Ras signalling activity was analysed by measuring the levels of Ras-GTP in unstimulated and TGF-β_1-stimulated cells (Figure 4). As expected, the basal level of active Ras-GTP was strikingly higher in PDV compared to MCA3D cells. TGF-β_1 induced a rapid and transient enhancement of Ras-GTP levels in both cell lines, without changing Ras protein expression. Maximal activation for both cell lines occurred at 2 min of treatment, and a decay to baseline levels at about 10 min (Figure 4a,b).

We also studied the activity of Erk by analysing the immunofluorescent localization of Erk proteins using an antibody that recognizes both Erk1 and Erk2 isoforms. Activation of Erk occurs in the cytoplasm and implies phosphorylation by MEK and translocation into the nucleus (Davis, 1993; Hill and Treisman, 1995). As shown in Figure 5a,b, Erk proteins were found mostly in the cytoplasm of unstimulated MCA3D and PDV cells, and only a small percentage of the cell population (below 5% in MCA3D and about 12% in PDV) exhibited Erk nuclear localization.
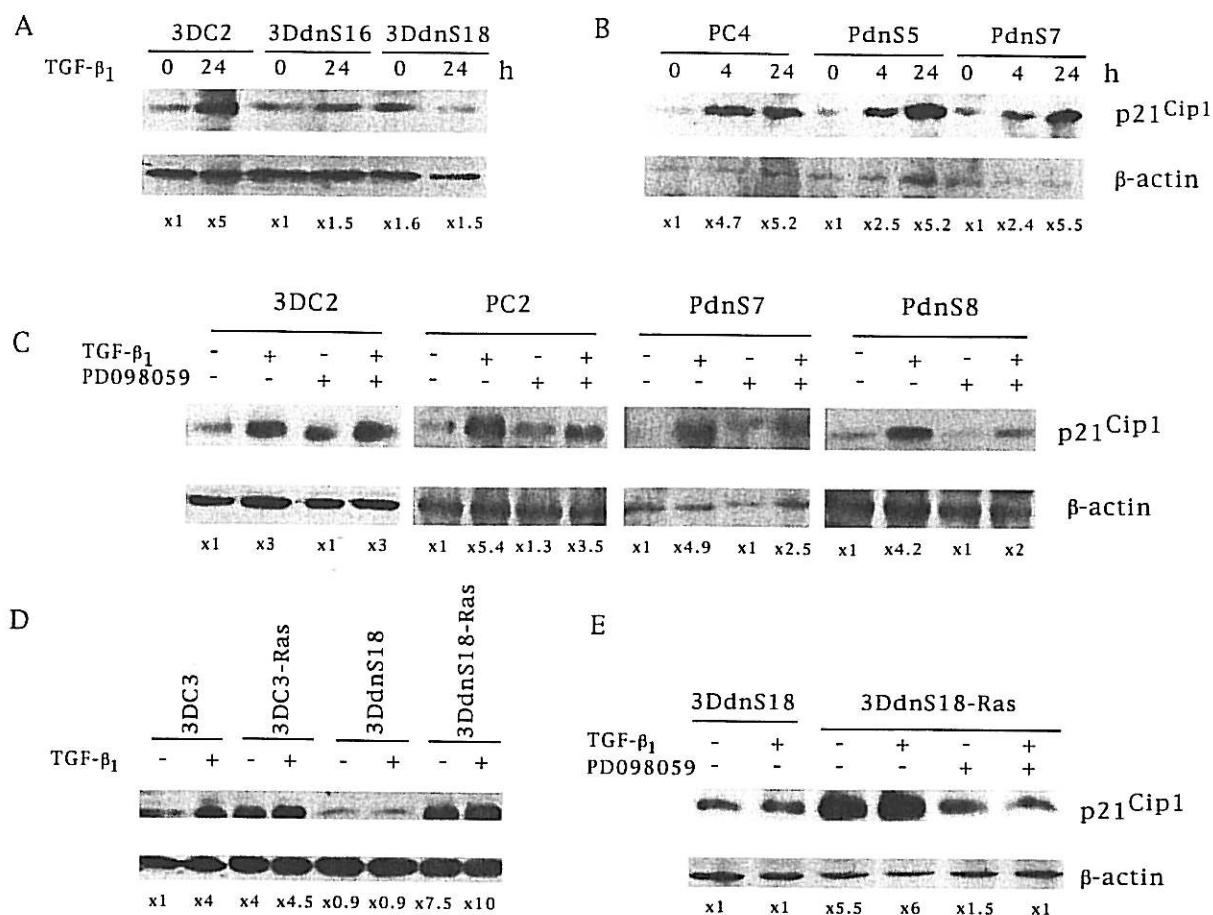
Figure 3 Induction of p21^{Cip1} protein expression by TGF-β_1 in MCA3D and PDV cell transfectants. Effect of PD098059 on TGF-β_1-stimulated p21^{Cip1} levels. (a, b) Lysates from synchronized cells grown in complete medium, untreated or treated with TGF-β_1 for the indicated time periods, were subjected to Western immunoblotting with an anti-p21^{Cip1} monoclonal antibody. The level of β-actin expression, as a protein loading control, was also determined. (c) p21^{Cip1} protein expression was determined in lysates from cells grown in medium minus serum, unstimulated or stimulated with TGF-β_1 for 24 h, in the absence or presence of 50 μM PD098059. The figure shows a representative experiment out of three. PD098059 inhibited induction of p21^{Cip1} by TGF-β_1 in PC and PdnS but not in 3DC2 cells. Similar results were obtained with the 3DC3 clone and with the parental cell line (not shown). (d, e) Infection of MCA3D control and dominant-negative Smad4 cell transfectants with oncogenic Ras induces p21^{Cip1}. (e) PD098059 inhibits Ras-induced p21^{Cip1} levels in 3DdnS18 cells. Similar results were obtained with 3DC-Ras clones (not shown). Stimulation with TGF-β_1 was in the absence (d) or presence (e) of serum. Quantitation of both p21^{Cip1} and β-actin was performed by densitometric analysis to correct for differences in loading. Values indicated at the bottom of auto-radiographs are expressed relative to untreated cells, in which an arbitrary value of 1 was given

The higher percentage of Erk nuclear accumulation in PDV cells indicated a certain constitutive activation of Erk signalling in basal conditions, consistent with the presence of elevated levels of Ras-GTP in this latter cell line. On TGF-β_1 addition, Erk proteins were transiently translocated into the nucleus in about 90% of both MCA3D and PDV cells, although with a slight difference in their kinetic profiles: Maximal nuclear accumulation occurred at 15–30 min (PDV) and 30–60 min (MCA3D), and the final slope of the kinetics was more pronounced in MCA3D cells (Figure 5a).

The effect of the MEK inhibitor PD098059 on TGF-β_1-induced nuclear translocation of Erk was analysed in PDV cells. Treatment of the cells with increasing concentrations of PD098059 resulted in a dose-dependent inhibition of Erk nuclear accumulation (Figure 5c). Inhibition was none at 10 μM, partial at 25 μM, and complete at 50 μM. TGF-β_1 stimulated the levels of phosphorylated Erk proteins, as shown in the Western blot of Figure 5d, in which a specific monoclonal antibody that recognizes the phosphorylated forms of both Erk1 and Erk2 was used. Increased

phosphorylation of Erk was more evident in Erk2, did not involve changes in Erk protein expression, and was inhibited by PD098059 at 50 μM (Figure 5d).

Blockade of Smad4 in transformed keratinocytes leads to hyperactivation of the Ras/Erk signalling pathway associated with increased secretion of urokinase and tumour progression

Thereafter, we analysed the nuclear localization of Erk proteins in the transfectants before and after a treatment of 30 min with TGF-β_1. Untreated PdnS clones consistently showed increased basal nuclear localization of Erk proteins (about 40% of the cells) respect to PC controls (about 10%); suggesting that the level of Erk signalling is further increased in PDV dominant-negative Smad4 cells. In contrast, the percentage of cells with Erk accumulated in the nucleus was similar (2–3%) in untreated 3DC and 3DdnS cells (Figure 6b), indicating that inhibition of Smad4 in non-transformed keratinocytes had no effect on the Erk pathway. TGF-β_1 stimulated nuclear translocation
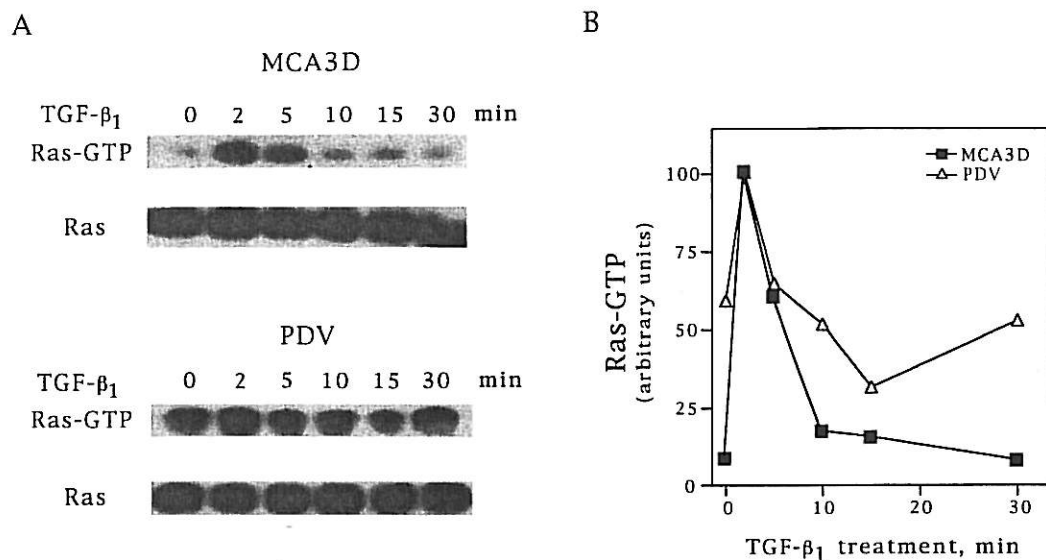
A

MCA3D

TGF-β_1 0   2   5   10   15   30   min

Ras-GTP

Ras

PDV

TGF-β_1 0   2   5   10   15   30   min

Ras-GTP

Ras

B

Figure 4   TGF-β_1 activates Ras in MCA3D and PDV cells. (a) Cells were stimulated with TGF-β_1 for different time periods (0–30 min). The levels of Ras-GTP were determined in the cell lysates (1.1 mg of total protein) by precipitating with RBD-Sepharose followed by Western immunoblotting with a pan-Ras monoclonal antibody. The level of Ras protein expression was also determined in the cell lysates. (b) Quantitation of the Ras-GTP levels of the experiment showed in (a) was performed by densitometric analysis. A representative experiment out of three is presented
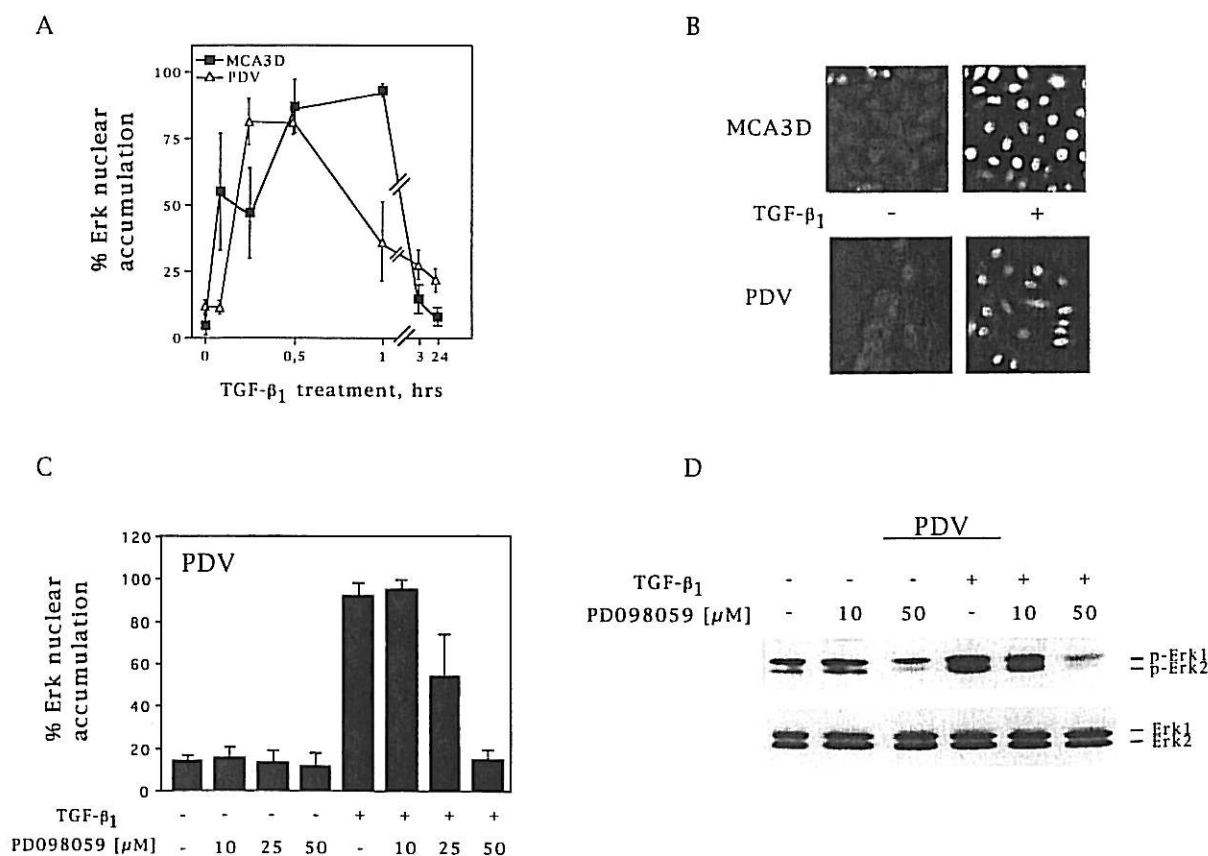
A

B

C

D

PDV

TGF-β_1 –   –   –   +   +   +
PD098059 [μM]   –   10   50   –   10   50

  = p-Erk1 / p-Erk2

  = Erk1 / Erk2

Figure 5   TGF-β_1 activates Erk signalling in MCA3D and PDV cells. Effect of the MEK inhibitor PD098059. (a, b) TGF-β_1-induced nuclear accumulation of Erk proteins in MCA3D and PDV cells. (a) MCA3D and PDV cells were stimulated with TGF-β_1 for different time periods (0–24 h) and Erk proteins localized by immunofluorescence analysis with a polyclonal antibody recognizing Erk1 and Erk2 isoforms. The percentage of cells with Erk predominantly or exclusively in the nucleus was determined as described in Materials and methods. (b) Immunolocalization of Erk proteins in unstimulated cells or cells stimulated with TGF-β_1 for 30 min. (c) TGF-β_1-induced nuclear accumulation of Erk1,2 in PDV cells is inhibited by PD098059. Unstimulated cells, or cells stimulated with TGF-β_1 for 30 min, were treated with different concentrations of PD098059, and the percentage of cells with Erk1,2 accumulated in the nucleus determined. Values represent the means ($\pm$s.d.) of counts from three independent experiments. (d) TGF-β_1 stimulates phosphorylation of Erk proteins in PDV cells. Effect of PD098059. Lysates from unstimulated cells, or from cells stimulated with TGF-β_1 for 30 min, untreated or treated with PD098059 at the indicated concentrations, were subjected to Western immunoblotting with antibodies recognizing total Erk1,2 proteins (bottom) or their phosphorylated forms (p-Erk)

A

% Erk nuclear accumulation

125
100
75
50
25
0

PC2 PC4 PdnS5 PdnS7 PdnS8

B

Ras   3DC4 3DC4-Ras

100
75
50
25
0

3DC2 3DC2-Ras 3DC4 3DC4-Ras 3DdnS18 3DdnS18-Ras

C

3DC2 3DC2+TGF-β1 3DdnS18 3DdnS18-Ras PC4 PdnS5 PdnS7 PdnS8

—p-Erk1
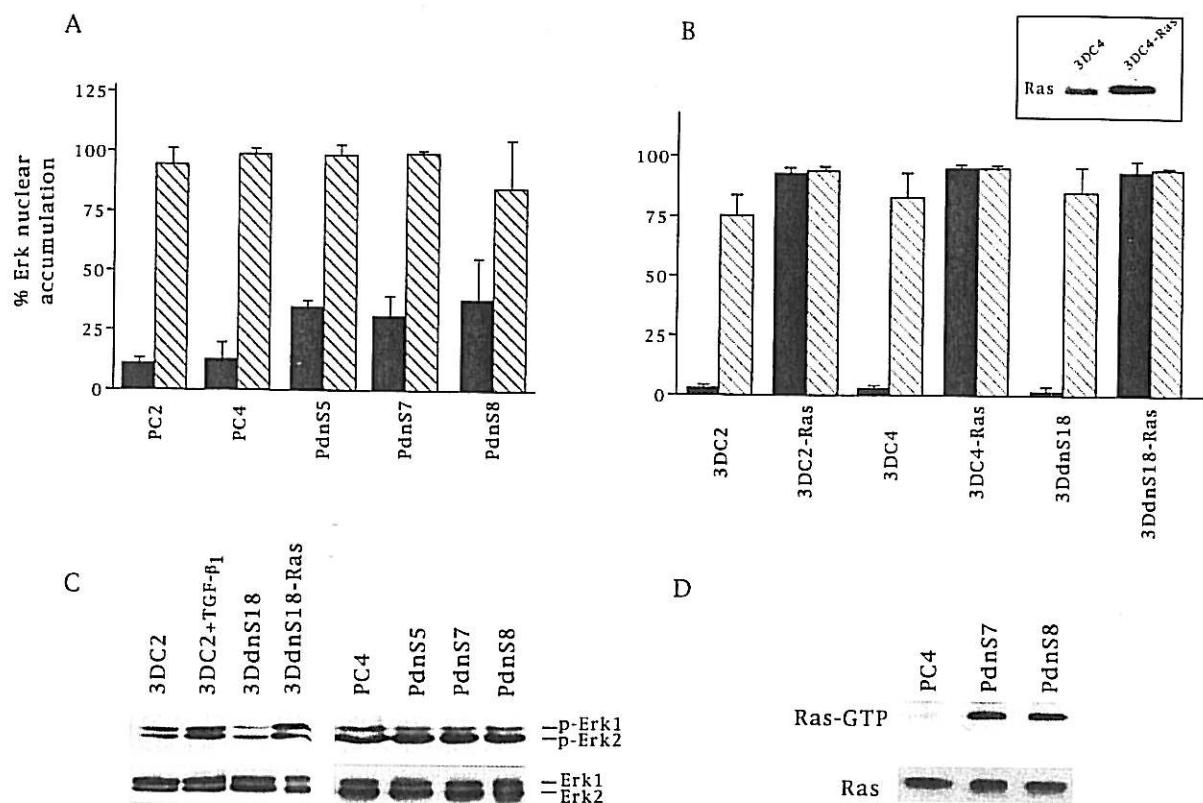—p-Erk2

=Erk1
Erk2

D

PC4 PdnS7 PdnS8

Ras-GTP

Ras

Figure 6 Comparison of Erk and Ras activation in control and dominant negative Smad4 cell transfectants. (a) Nuclear accumulation of Erk in PDV cell transfectants unstimulated (black bars) or stimulated with TGF-β_1 (diagonally striped bars) for 30 min. (b) Nuclear accumulation of Erk in non-infected and Ras-infected MCA3D cell transfectants unstimulated or stimulated with TGF-β_1 as above. Ras-infected cells express relatively high levels of viral Ras proteins, which migrate with a slightly lower mobility than endogenous normal Ras proteins in polyacrylamide gels, as shown by Western immunoblotting with a pan-Ras monoclonal antibody (insert). (c) Erk phosphorylation levels in different cell lines. The relative levels of total and phosphorylated Erk1 and Erk2 proteins were determined as in the legend to Figure 5d. (d) Comparison of Ras activation in PDV cell transfectants. The levels of Ras bound to GTP and Ras protein expression were determined in the cell lysates (0.7 mg of total protein) as in the legend of Figure 4

of Erk at the same extent (90–100%) in all clones (Figure 6a,b). In Ras-infected 3DC and 3DdnS cells, nuclear accumulation of Erk raised maximum levels in basal conditions, masking the effect of TGF-β_1 (Figure 6b). As expected, low levels of phospho-Erk1,2 proteins were found in 3DC and 3DdnS cells. Phosphorylation of both isoforms increased after infection with Ras or stimulation with TGF-β_1 (Figure 6c). In contrast, enhanced levels of phospho-Erk2, but not of phospho-Erk1, were observed in unstimulated PdnS transfectants compared with control PC4 cells (Figure 6c). We also analysed the activity of Ras signalling by comparing the levels of Ras-GTP in PC and PdnS transfectants. PdnS7 and PdnS8 cells showed elevated levels of Ras-GTP respect to control PC4 cells, and this enhancement was not due to increased Ras protein expression (Figure 6d). The same result was obtained with PdnS5 (not shown). These findings are consistent with the idea that inhibition of Smad4 in transformed PDV keratinocytes leads to a constitutive hyperactivation of the Ras/Erk transduction pathway mediated by phosphorylation of Erk2.

Treatment of PDV cells with TGF-β_1 up-regulates uPA expression/secretion associated with stimulation of cell motility and invasiveness (Santibáñez et al., 1999). We show in another report that stimulation of uPA production by TGF-β_1 in PDV cells requires the Ras/Erk signalling pathway (Santibáñez et al., 2000).

Interestingly, PdnS clones consistently secreted increased amounts of uPA compared with control clones (Figure 7a) or the parental cell line (not shown). Treatment with TGF-β_1 for 24 h stimulated uPA production about threefold in PC cells and slightly enhanced the levels of uPA secreted by some PdnS clones (Figure 7a,b). Both basal and TGF-β_1-induced levels of uPA secreted by PdnS cells were inhibited by PD098059 at 50 μM, which also reduced uPA secretion in TGF-β_1-stimulated PC cells, as exemplified with PdnS8 and PC4 clones in Figure 7b. Nevertheless, dominant-negative 3DdnS cells did not increase basal secretion of uPA respect to the parental cell line (Figure 7c) or control clones (not shown). In unstimulated MCA3D cells, secreted uPA was enhanced by overexpression of oncogenic Ras after retroviral infection, and this increase was also inhibited by PD098059 (Figure 7c). The same result was obtained in 3DdnS cells (not shown).

To analyse whether enhanced secretion of uPA in PdnS clones correlated with increased motility, we performed an in vitro wound healing assay comparing the abilities of PC and PdnS clones to repopulate a wound made 24 h before (Figure 8a,b). PdnS clones showed higher migratory abilities than PC in unstimulated conditions. TGF-β_1 enhanced cell motility of all clones, although the effect was more pronounced in control PC cells. To demonstrate the involvement of

Blockade of Smad4 in transformed keratinocytes containing a Ras oncogene leads to hyperactivation of the Ras-dependent Erk signalling pathway associated with progression to undifferentiated carcinomas

Maite Iglesias[1], Pilar Frontelo[1], Carlos Gamallo[2] and Miguel Quintanilla*[,1]

[1]Instituto de Investigaciones Biomédicas Alberto Sols CSIC-UAM, Arturo Duperier 4, 28029-Madrid, Spain; [2]Hospital de la Princesa, Departamento de Anatomía Patológica, Facultad de Medicina, UAM, 28029-Madrid, Spain

Smad4 functions as a transcription factor in TGF-β signalling. We have investigated the role of Smad4 in the TGF-β_1 cell responses of transformed PDV keratinocytes, which contain a Ras oncogene, and of non-tumorigenic MCA3D keratinocytes, by transfecting both cell lines with a dominant-negative Smad4 construct. Smad4 mediates TGF-β_1-induced up-regulation of p21^{Cip1} and growth arrest in MCA3D cells. However, in PDV keratinocytes, Smad4 is only partially involved in TGF-β_1-induced growth inhibition, and does not mediate enhancement of p21^{Cip1} levels by the growth factor. TGF-β_1 activates Ras/Erk signalling activity in both cell lines. PD098059, a specific inhibitor of MEK, diminishes TGF-β_1-induced p21^{Cip1} levels in PDV but not in MCA3D cells, suggesting an involvement of Erk in up-regulation of p21^{Cip1} by TGF-β_1 in PDV cells. PDV dominant-negative Smad4 cell transfectants, but not MCA3D transfectants, showed constitutive hyperactivation of the Ras/Erk signalling pathway, increased secretion of urokinase, higher motility properties, and a change to a fibroblastoid cell morphology associated *in vivo* with the transition from a well differentiated to a poorly differentiated tumour phenotype. Infection of MCA3D control and dominant negative Smad4 cell transfectants with retroviruses carrying a Ras oncogene led to enhanced p21^{Cip1} and urokinase secreted levels, independently of TGF-β_1 stimulation, that were reduced by PD098059. These results suggest that Smad4 acts inhibiting Ras-dependent Erk signalling activity in Ras-transformed keratinocytes. Loss of Smad4 function in these cells results in hyperactivation of Erk signalling and progression to undifferentiated carcinomas. *Oncogene* (2000) **19**, 4134–4145.

Keywords: TGF-β_1; Smad4; Ras; Erk; urokinase; carcinoma

Introduction

Transforming growth factor-β (TGF-β) regulates cell proliferation, differentiation, motility, adhesion, and death in most tissues, including epithelia (Massagué, 1990; Lahio and Keski-Oja, 1992). During the last years the idea of a dual function of TGF-β in epithelial carcinogenesis has gained considerable support. TGF-β acts as a suppressor of tumour formation by virtue of its role in inhibiting proliferation of epithelial cells (Alexandrow and Moses, 1995; Massagué, 1998), but it also stimulates malignant progression at later stages of tumorigenesis by inducing an epithelial-mesenchymal transition associated with the development of a highly aggressive undifferentiated type of tumour (Caulin *et al.*, 1995; Cui *et al.*, 1996; Oft *et al.*, 1996, 1998; Frontelo *et al.*, 1998; Portella *et al.*, 1998).

Studies on the mouse skin carcinogenesis model and on mammary epithelial cells suggest a synergistic co-operation between oncogenic Ras and TGF-β_1 to stimulate malignant progression (Oft *et al.*, 1996; Akhurst and Balmain, 1999). The effects of the growth factor on carcinoma cell invasiveness and metastasis appear to be direct and require signalling through the type II receptor (Oft *et al.*, 1998; Portella *et al.*, 1998).

TGF-β signals through formation of heteromeric complexes between type I and type II serine/threonine kinase receptors. After activation, the signal transducing type I receptor binds and phosphorylates Smad2, Smad3 proteins that associate with Smad4 in the cytoplasm, and these complexes, then, translocate into the nucleus in which they activate transcription of specific genes (see Massagué, 1998; Zhang and Derynck, 1999; for reviews). TGF-β signalling components, such as type II receptors and Smad proteins, have been shown to be inactivated by mutation or deletion in human cancers (Massagué, 1998). Particularly, Smad4 (DPC4) was originally identified as a tumour suppressor gene frequently inactivated in pancreatic and colon carcinomas. Reconstitution of Smad4 in colon carcinoma defective cells leads to suppression of tumorigenicity (Schwarte-Waldhoff *et al.*, 1999)

Several reports point to a rapid and direct activation of the Ras-mitogen-activated protein (MAP) kinase signalling pathway associated with growth inhibition by TGF-β in epithelial cells (Hartsough *et al.*, 1996; reviewed in Hartsough and Mulder, 1997). The growth inhibitory response to TGF-β appears to be mediated by induction of cyclin-dependent kinase (cdk) inhibitors, such as p21^{Cip1} and p15^{INK4B} (Datto *et al.*, 1995; Hannon and Beach, 1994; Reynisdóttir *et al.*, 1995). The signalling pathways involved in these TGF-β-induced gene responses remain an open question (see Massagué, 1998). Thus, p21^{Cip1} appears to be a downstream target gene regulated by Smad4 in carcinoma cells (Grau *et al.*, 1997; Hunt *et al.*, 1998), while it has been reported that Ras and the MAP kinase pathway are required for up-regulation of p21^{Cip1} by TGF-β in intestinal epithelial cells and human keratinocytes, respectively (Yue *et al.*, 1998; Hu

et al., 1999). The same appears to occur for TGF-β-mediated induction of other genes, such as the 3TP-lux reporter construct, which contains a known TGF-β-inducible plasminogen activator inhibitor-1 (PAI-1) promoter (Grau *et al.*, 1997; Mucsi *et al.*, 1996; de Winter *et al.*, 1997). This scenario has been complicated as several reports demonstrate a cross-talk between the Smad and Ras-MAP kinase signalling pathways (reviewed in Zhang and Derynck, 1999). Recently, Kretzschmar *et al.* (1999) found that oncogenic Ras, acting via MAP kinases, inhibits TGF-β-induced nuclear accumulation of Smad2 and Smad3. However, another report has shown that constitutively active MEK, or inhibitors for MEK, have no effect on Smad activity in human keratinocytes (Hu *et al.*, 1999).

In this work, we have analysed the role of Smad4 in the TGF-β_1 responses of immortalized (MCA3D) and transformed (PDV) mouse epidermal keratinocytes by transfecting both cell lines with a C-terminal truncated, dominant-negative, Smad4 construct (Lagna *et al.*, 1996). MCA3D cells are non-tumorigenic and exhibit normal Ras and p53 genes, while PDV are chemically transformed keratinocytes and produce low metastatic well differentiated squamous cell carcinomas upon injection in mice (Caulín *et al.*, 1995; Frontelo *et al.*, 1998). PDV cells contain a mutated H-Ras gene and express relatively low levels of activated Ras proteins (Quintanilla *et al.*, 1991). They also have inactivated p53 loci (Burns *et al.*, 1991). Both cell lines are growth-inhibited by TGF-β_1, but they respond differentially to chronic treatment with the growth factor. While MCA3D cells are induced to terminal differentiation and cell death in response to TGF-β_1, the growth factor stimulates cell motility and invasiveness in PDV cells, which undergo a reversible epithelial-mesenchymal conversion linked to progression toward a metastatic poorly differentiated tumour phenotype (Caulín *et al.*, 1995; Frontelo *et al.*, 1998). The invasive response of PDV and other carcinoma cells to TGF-β_1 is associated with enhanced expression/secretion of urokinase (uPA) and of its inhibitor PAI-1 (Farina *et al.*, 1998; Santibáñez *et al.*, 1999). uPA is a serine proteinase that converts the inactive plasminogen into the broad-spectrum active proteinase plasmin, which in turn degrades many proteins of the extracellular matrix and activates other matrix metalloproteinases (Andreasen *et al.*, 1997).

We show that inhibiting Smad4 in Ras-transformed keratinocytes leads to hyperactivation of the Ras/Erk signalling pathway, increased secretion of uPA, and progression to a poorly differentiated tumour phenotype. On the other hand, a switch between the Smad and Erk signalling pathways, depending on the presence of oncogenic Ras, appears to occur in keratinocytes to mediate induction of p21[Cip1] by TGF-β_1.

Results

Smad4 mediates growth inhibition in both MCA3D and PDV keratinocytes

MCA3D and PDV cell lines were transfected either with a full-length Smad4 cDNA or with a C-terminal truncated dominant-negative Smad4 (1–514) construct, together with the pcDNA3 neomycine resistant vector. Previously, the presence of Smad4 transcripts in both cell lines was demonstrated by RT–PCR (data not shown). After transfection with the normal full-length cDNA, no viable clones were obtained from MCA3D cells; while several clones could be selected up to the third passage, in which they died, in the case of PDV cells. These results suggest that overexpression of Smad4 induces cell death in keratinocytes, as reported for other epithelial cells (Atfi *et al.*, 1997), although this hypothesis was not further investigated. Stable clones transfected with the dominant-negative Smad4 (1–514) construct were isolated from both MCA3D and PDV cell lines (designated as 3DdnS and PdnS, respectively). Clones transfected with the pcDNA3 vector alone were also obtained (designated as 3DC and PC) to be used as controls.

The activity of Smad signalling in the transfectants was analysed by measuring TGF-β_1-induced nuclear accumulation of Smad2/Smad3 in immunofluorescence experiments using a specific anti-Smad2,3 antibody (Figure 1). In exponentially growing MCA3D and PDV cells, untreated with TGF-β_1, anti-Smad2,3 staining was predominantly cytoplasmic concentrated at the perinuclear region, although about 18% of the cells showed Smad2/Smad3 accumulated in the nucleus (Figure 1a,b). This percentage of unstimulated cells with Smad2,3 localized into the nucleus was probably as consequence of TGF-β factors present in the serum or secreted by their own cells. In any case, on addition of TGF-β_1, about 90% of MCA3D cells showed anti-Smad2,3 staining concentrated into the nucleus. This response was rapid, with a maximum at 20 min, and lasted for about 1 h (Figure 1b). PDV cells responded partially to TGF-β_1-induced nuclear translocation of Smad2,3. Anti-Smad2,3 nuclear staining was limited to about 40% of the cells at 30 min of treatment (Figure 1a,b), indicating a constitutive inhibition of Smad signalling in these transformed keratinocytes, likely because of the presence of a Ras oncogene (Kretzschmar *et al.*, 1999). 3DdnS and PdnS transfectants did not respond to TGF-β_1 for nuclear accumulation of Smad2,3 (see in Figure 1c the results obtained with 3DdnS18, PdnS7 and PdnS8; other clones, such as 3DdnS16, 3DdnS17 and PdnS5, behaved similarly), while nuclear translocation of Smad proteins was stimulated in control clones as in the corresponding parental cell lines (not shown). These results clearly indicated that the Smad transduction pathway was blocked in the dominant-negative Smad4 transfectants.

Although MCA3D cells are most sensitive than PDV for TGF-β_1-induced growth inhibition, both cell lines are growth-inhibited by concentrations of TGF-β_1 above 1 ng/ml (Haddow *et al.*, 1991). As shown in Figure 2, TGF-β_1, at 10 ng/ml, inhibited the growth of 3DC and PC control cell clones after 48 h of treatment. All of the dominant-negative Smad4 transfectant clones showed resistance to growth inhibition, but, while it was drastically reduced in 3DdnS cells (Figure 2a), a significant inhibition of growth was still induced by TGF-β_1 in PdnS clones (Figure 2b), suggesting that other signalling pathways, in addition to Smad, could be involved in the antiproliferative response of transformed keratinocytes to TGF-β_1.
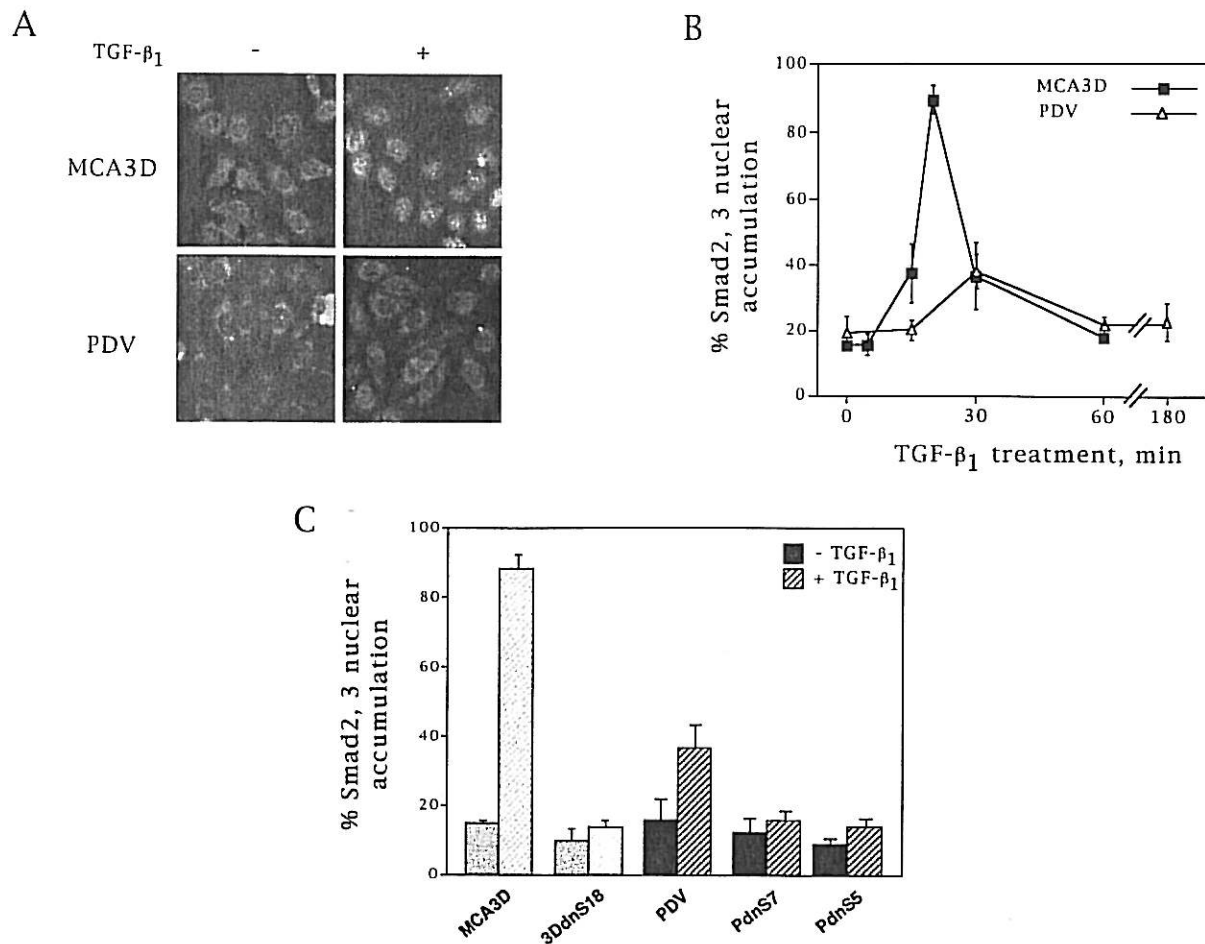
Figure 1 TGF-β_1-induced nuclear accumulation of Smad2/Smad3 in MCA3D and PDV cells, and in dominant-negative Smad4 transfectants. (a) Endogenous Smad2 and Smad3 were visualized by anti-Smad2,3 immunofluorescence staining in MCA3D and PDV cells untreated or treated with TGF-β_1 for 20 min and 30 min, respectively. (b) MCA3D and PDV cells were treated with TGF-β_1 for different time periods. Following immunofluorescence staining, the percentage of cells with Smad2,3 staining concentrated in the nucleus was calculated as described in Materials and methods. (c) Nuclear accumulation of Smad2,3 in response to TGF-β_1 in MCA3D, PDV and dominant-negative Smad4 transfectants. Treatments with the growth factor were of 20 min for MCA3D and 3DdnS18, and of 30 min for PDV, PdnS7 and PdnS5

We also analysed the activation by TGF-β_1 of 3TP-lux, a TGF-β-inducible reporter gene containing a PAI-1 promoter. Previous results indicated that TGF-β_1 induced a twofold activation of 3TP-lux in PDV cells after 24 h of treatment, while MCA3D cells were unable to respond to the growth factor for PAI-1 induction (Santibáñez et al., 1999). As shown in Figure 2c, TGF-β_1 activated 3TP-lux in the control PC2 clone (about twofold), while no significant activation of the reporter gene was found in PdnS transfectants. This result indicates that Smad4 is a key element in the TGF-β signal transduction cascade in transformed keratinocytes.

Smad4 mediates up-regulation of p21^Cip1 by TGF-β_1 in MCA3D, but not in PDV cells in which the Erk signalling pathway is required

It has been demonstrated that TGF-β_1 induces the expression of the cdk inhibitor p21^Cip1 in normal and transformed keratinocytes, and that induction of p21^Cip1, together with alterations in other cell cycle regulatory molecules, seems to be partially responsible of the growth-inhibitory effects of TGF-β_1 (Malliri et al., 1996). We studied the expression of

p21^Cip1 in control and dominant-negative Smad4 cell transfectants by Western blot analysis of cell extracts obtained from synchronous exponentially growing cultures, untreated or treated with TGF-β_1 (Figure 3). No significant differences for induction of p21^Cip1 in response to TGF-β_1 were observed when cells were cultured in the presence or absence of serum, although the basal protein levels of p21^Cip1 (relative to the expression of β-actin, used as a protein loading marker) were higher when serum was present. Exposure to TGF-β_1 resulted in a fivefold induction of p21^Cip1 protein expression in 3DC and PC control clones (Figure 3a–c). This response was blocked in 3DdnS transfectants (Figure 3a), while no differences for TGF-β_1 up-regulation of p21^Cip1 were observed between control PC and dominant-negative PdnS transfectants (Figure 3b,c). Since the Erk MAP kinase signalling pathway has also been implicated in the regulation of p21^Cip1 by TGF-β in epithelial cells (Yue et al., 1998; Hu et al., 1999), we studied the effects of PD098059, a specific inhibitor of MAP kinase kinase (MEK) (Simon et al., 1996), on p21^Cip1 protein induction by TGF-β_1. PD098059, at a concentration of 50 μM (that is shown to inhibit efficiently Erk signalling activity in PDV cells, see
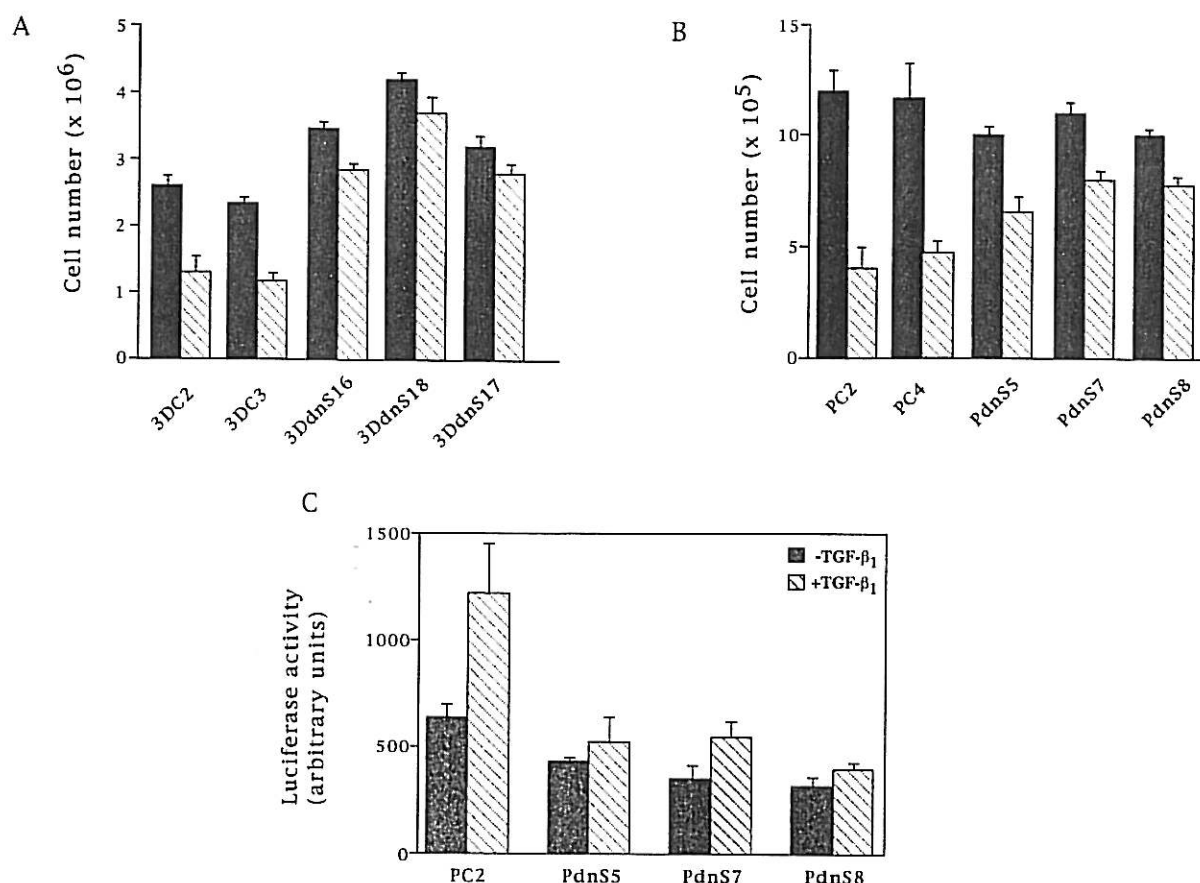
Figure 2 TGF-β_1-induced growth inhibition and transcriptional activation of the 3TP-lux reporter in the cell transfectants. (a, b) Cell growth inhibition assays in control (3DC, PC) and dominant-negative Smad4 (3DdnS, PdnS) transfectants. Synchronized cells, about 1×10^6 cells in (a) and 4.5×10^5 cells in (b), were seeded in 20-cm^2 culture dishes and grown in medium plus serum. TGF-β_1 treatment started on the following day. After 48 h, cells on TGF-β_1-treated (diagonally stripped bars) and untreated (black bars) dishes were counted. The figures represent the means ($\pm$s.d.) of quadruplicate incubations. (c) Induction of 3TP-lux by TGF-β_1 in PDV cell transfectants. Cells were transiently transfected with the 3TP-lux reporter plasmid and incubated without or with TGF-β_1 for 24 h. Luciferase activity in the cell lysates, corrected for transfection efficiency as indicated in Materials and methods, was plotted as the average (and s.d.) for duplicate determinations of two independent experiments

below), consistently reduced (by 35–50%) TGF-β_1-stimulated p21^{Cip1} expression in PC and PdnS clones, while it did not affect the enhancement of p21^{Cip1} by the growth factor in 3DC cells (Figure 3c). Altogether, these data indicated that Smad4 does not mediate regulation of p21^{Cip1} protein levels by TGF-β_1 in transformed PDV keratinocytes, and that this response appeared to require Erk MAP kinase signalling activity.

To study whether the expression of oncogenic Ras could explain the involvement of Erk in the modulation of p21^{Cip1} levels by TGF-β_1 in PDV cells, we infected 3DC and 3DdnS transfectants with retroviruses carrying an activated H-Ras gene, and analysed the levels of p21^{Cip1} in the absence and presence of TGF-β_1. Infection of the cells with the Harvey murine sarcoma virus (HMSV) produced a relatively high level of oncogenic Ras protein expression (see below), and resulted in a strong basal induction (4–7-fold) of p21^{Cip1} protein levels (Figure 3d,e). This increase was similar to that induced by TGF-β_1 in non-infected 3DC cells (Figure 3d), and occurred in both control and dominant-negative Smad4 transfectants. p21^{Cip1} protein levels in Ras-infected cells were significantly reduced by treatment with PD098059 (Figure 3e).

TGF-β_1 induces a rapid and transient activation of Ras and Erk in MCA3D and PDV keratinocytes

Therefore, we studied whether TGF-β_1 was able to activate the Ras/Erk signalling pathway in MCA3D and PDV keratinocytes. Ras signalling activity was analysed by measuring the levels of Ras-GTP in unstimulated and TGF-β_1-stimulated cells (Figure 4). As expected, the basal level of active Ras-GTP was strikingly higher in PDV compared to MCA3D cells. TGF-β_1 induced a rapid and transient enhancement of Ras-GTP levels in both cell lines, without changing Ras protein expression. Maximal activation for both cell lines occurred at 2 min of treatment, and a decay to baseline levels at about 10 min (Figure 4a,b).

We also studied the activity of Erk by analysing the immunofluorescent localization of Erk proteins using an antibody that recognizes both Erk1 and Erk2 isoforms. Activation of Erk occurs in the cytoplasm and implies phosphorylation by MEK and translocation into the nucleus (Davis, 1993; Hill and Treisman, 1995). As shown in Figure 5a,b, Erk proteins were found mostly in the cytoplasm of unstimulated MCA3D and PDV cells, and only a small percentage of the cell population (below 5% in MCA3D and about 12% in PDV) exhibited Erk nuclear localization.
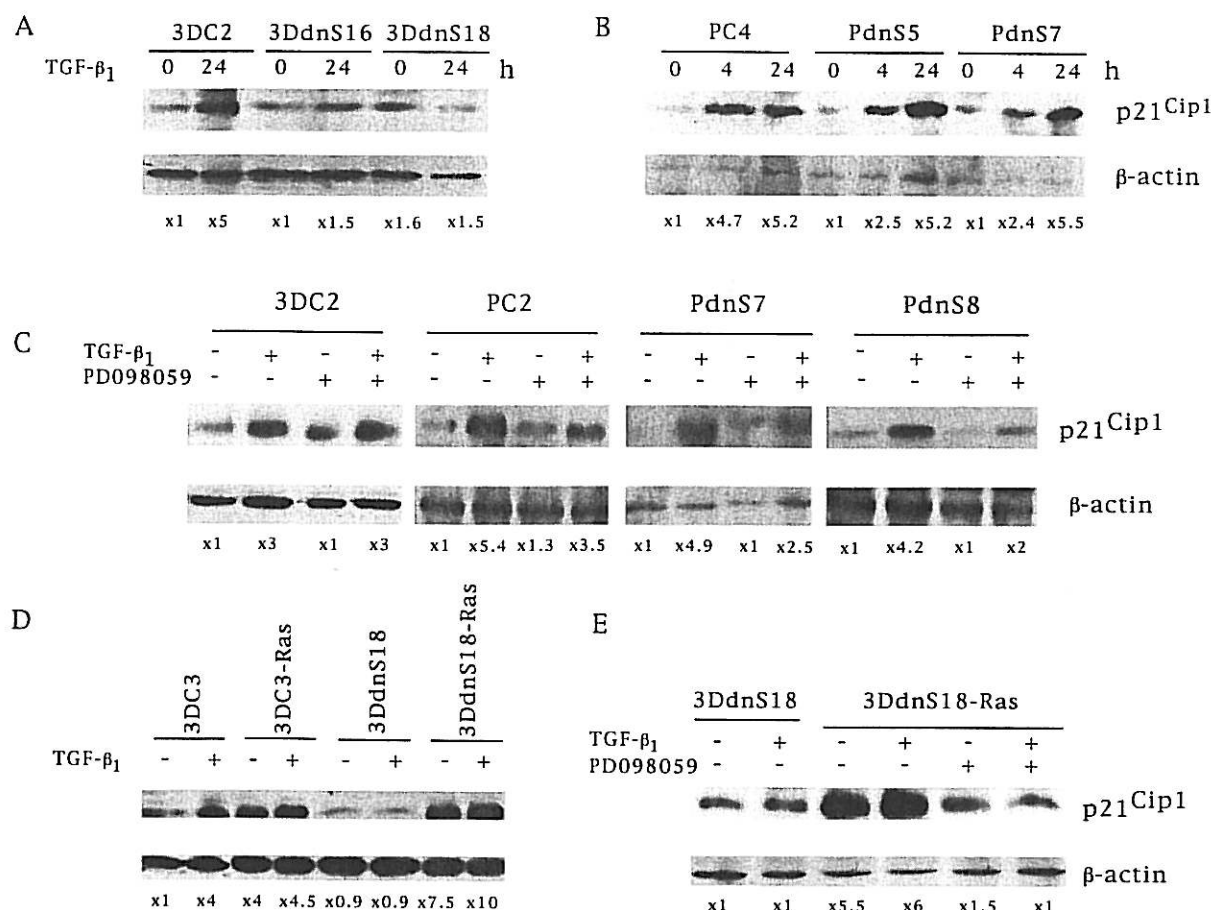
Figure 3 Induction of p21^{Cip1} protein expression by TGF-β_1 in MCA3D and PDV cell transfectants. Effect of PD098059 on TGF-β_1-stimulated p21^{Cip1} levels. (a, b) Lysates from synchronized cells grown in complete medium, untreated or treated with TGF-β_1 for the indicated time periods, were subjected to Western immunoblotting with an anti-p21^{Cip1} monoclonal antibody. The level of β-actin expression, as a protein loading control, was also determined. (c) p21^{Cip1} protein expression was determined in lysates from cells grown in medium minus serum, unstimulated or stimulated with TGF-β_1 for 24 h, in the absence or presence of 50 μM PD098059. The figure shows a representative experiment out of three. PD098059 inhibited induction of p21^{Cip1} by TGF-β_1 in PC and PdnS but not in 3DC2 cells. Similar results were obtained with the 3DC3 clone and with the parental cell line (not shown). (d, e) Infection of MCA3D control and dominant-negative Smad4 cell transfectants with oncogenic Ras induces p21^{Cip1}. (e) PD098059 inhibits Ras-induced p21^{Cip1} levels in 3DdnS18 cells. Similar results were obtained with 3DC-Ras clones (not shown). Stimulation with TGF-β_1 was in the absence (d) or presence (e) of serum. Quantitation of both p21^{Cip1} and β-actin was performed by densitometric analysis to correct for differences in loading. Values indicated at the bottom of auto-radiographs are expressed relative to untreated cells, in which an arbitrary value of 1 was given

The higher percentage of Erk nuclear accumulation in PDV cells indicated a certain constitutive activation of Erk signalling in basal conditions, consistent with the presence of elevated levels of Ras-GTP in this latter cell line. On TGF-β_1 addition, Erk proteins were transiently translocated into the nucleus in about 90% of both MCA3D and PDV cells, although with a slight difference in their kinetic profiles: Maximal nuclear accumulation occurred at 15–30 min (PDV) and 30–60 min (MCA3D), and the final slope of the kinetics was more pronounced in MCA3D cells (Figure 5a).

The effect of the MEK inhibitor PD098059 on TGF-β_1-induced nuclear translocation of Erk was analysed in PDV cells. Treatment of the cells with increasing concentrations of PD098059 resulted in a dose-dependent inhibition of Erk nuclear accumulation (Figure 5c). Inhibition was none at 10 μM, partial at 25 μM, and complete at 50 μM. TGF-β_1 stimulated the levels of phosphorylated Erk proteins, as shown in the Western blot of Figure 5d, in which a specific monoclonal antibody that recognizes the phosphorylated forms of both Erk1 and Erk2 was used. Increased

phosphorylation of Erk was more evident in Erk2, did not involve changes in Erk protein expression, and was inhibited by PD098059 at 50 μM (Figure 5d).

Blockade of Smad4 in transformed keratinocytes leads to hyperactivation of the Ras/Erk signalling pathway associated with increased secretion of urokinase and tumour progression

Thereafter, we analysed the nuclear localization of Erk proteins in the transfectants before and after a treatment of 30 min with TGF-β_1. Untreated PdnS clones consistently showed increased basal nuclear localization of Erk proteins (about 40% of the cells) respect to PC controls (about 10%); suggesting that the level of Erk signalling is further increased in PDV dominant-negative Smad4 cells. In contrast, the percentage of cells with Erk accumulated in the nucleus was similar (2–3%) in untreated 3DC and 3DdnS cells (Figure 6b), indicating that inhibition of Smad4 in non-transformed keratinocytes had no effect on the Erk pathway. TGF-β_1 stimulated nuclear translocation

A

MCA3D

TGF-β₁   0   2   5   10 15 30 min
Ras-GTP

Ras

PDV
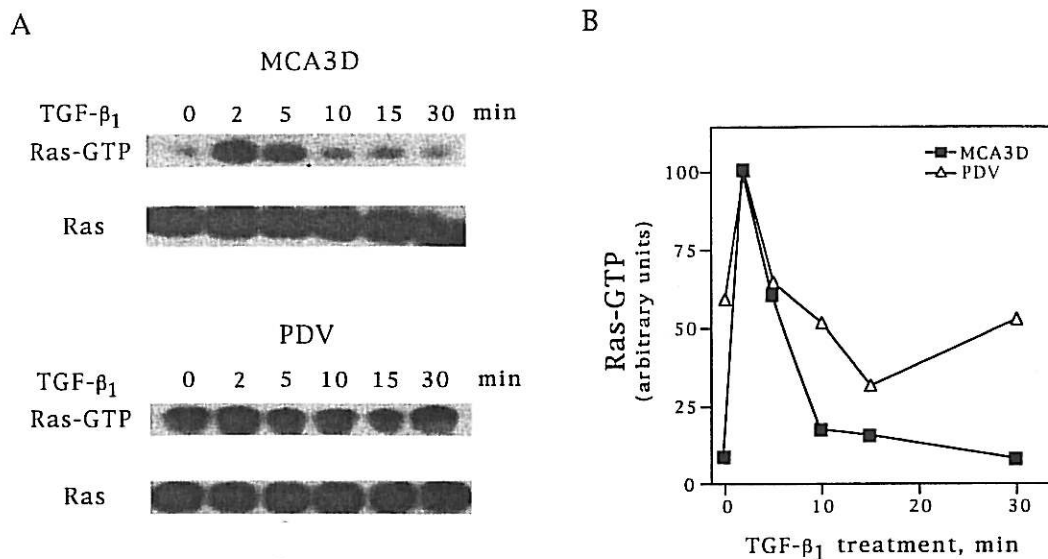
TGF-β₁   0   2   5   10 15 30 min
Ras-GTP

Ras

B

Figure 4 TGF-β₁ activates Ras in MCA3D and PDV cells. (a) Cells were stimulated with TGF-β₁ for different time periods (0–30 min). The levels of Ras-GTP were determined in the cell lysates (1.1 mg of total protein) by precipitating with RBD-Sepharose followed by Western immunoblotting with a pan-Ras monoclonal antibody. The level of Ras protein expression was also determined in the cell lysates. (b) Quantitation of the Ras-GTP levels of the experiment showed in (a) was performed by densitometric analysis. A representative experiment out of three is presented
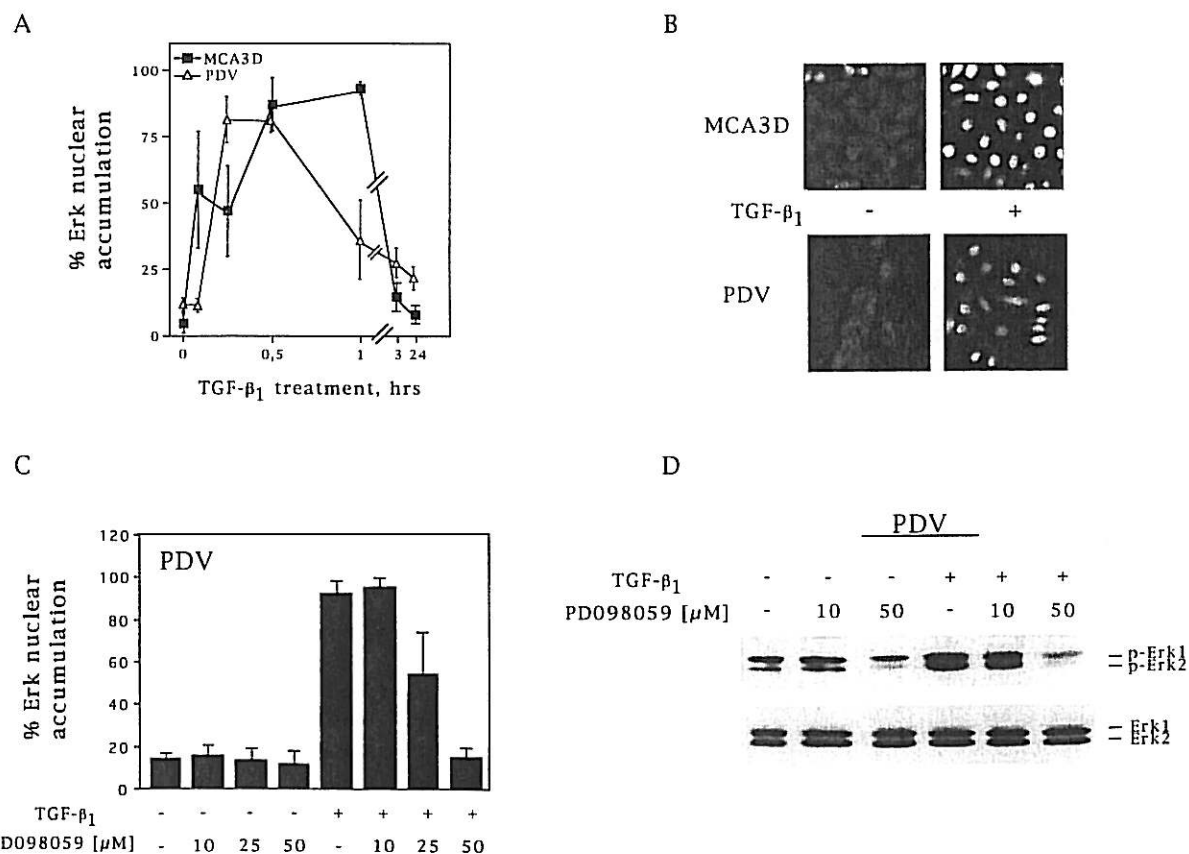
A

B

C

D

Figure 5 TGF-β₁ activates Erk signalling in MCA3D and PDV cells. Effect of the MEK inhibitor PD098059. (a, b) TGF-β₁-induced nuclear accumulation of Erk proteins in MCA3D and PDV cells. (a) MCA3D and PDV cells were stimulated with TGF-β₁ for different time periods (0–24 h) and Erk proteins localized by immunofluorescence analysis with a polyclonal antibody recognizing Erk1 and Erk2 isoforms. The percentage of cells with Erk predominantly or exclusively in the nucleus was determined as described in Materials and methods. (b) Immunolocalization of Erk proteins in unstimulated cells or cells stimulated with TGF-β₁ for 30 min. (c) TGF-β₁-induced nuclear accumulation of Erk1,2 in PDV cells is inhibited by PD098059. Unstimulated cells, or cells stimulated with TGF-β₁ for 30 min, were treated with different concentrations of PD098059, and the percentage of cells with Erk1,2 accumulated in the nucleus determined. Values represent the means (±s.d.) of counts from three independent experiments. (d) TGF-β₁ stimulates phosphorylation of Erk proteins in PDV cells. Effect of PD098059. Lysates from unstimulated cells, or from cells stimulated with TGF-β₁ for 30 min, untreated or treated with PD098059 at the indicated concentrations, were subjected to Western immunoblotting with antibodies recognizing total Erk1,2 proteins (bottom) or their phosphorylated forms (p-Erk)
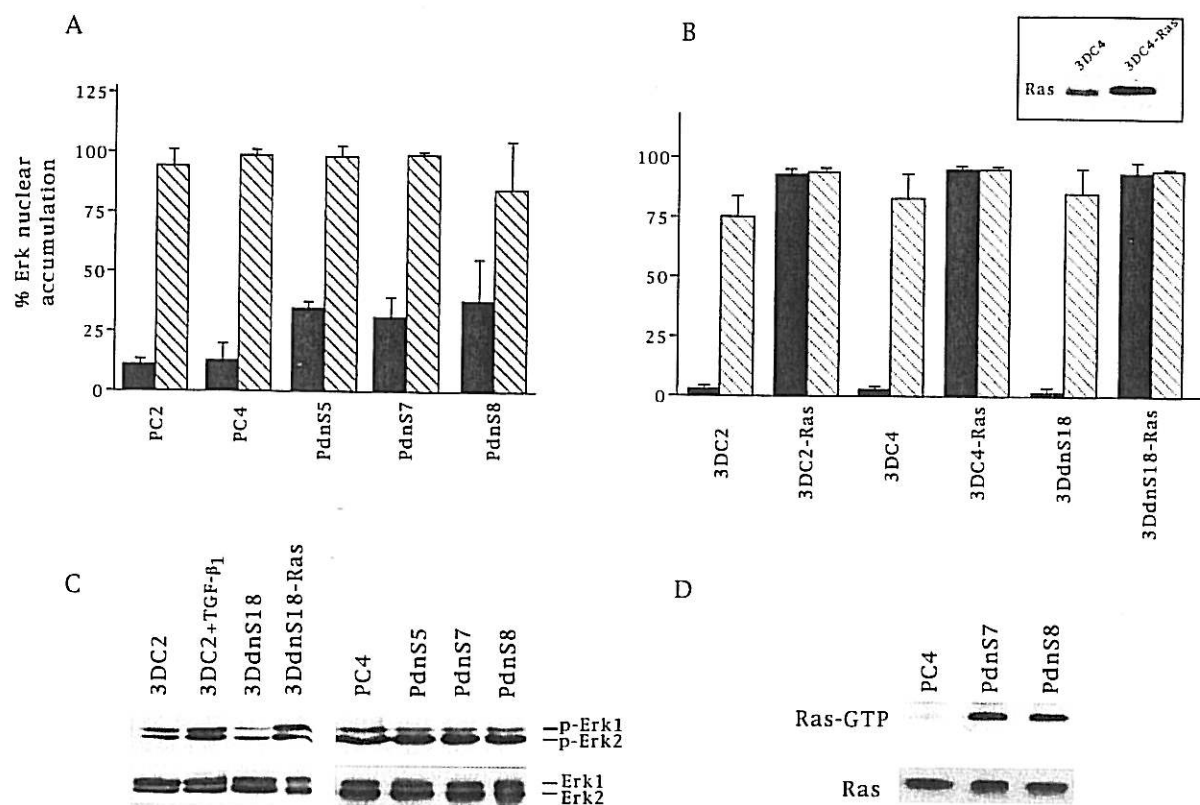
A

B

C

D

Figure 6 Comparison of Erk and Ras activation in control and dominant negative Smad4 cell transfectants. (a) Nuclear accumulation of Erk in PDV cell transfectants unstimulated (black bars) or stimulated with TGF-β_1 (diagonally striped bars) for 30 min. (b) Nuclear accumulation of Erk in non-infected and Ras-infected MCA3D cell transfectants unstimulated or stimulated with TGF-β_1 as above. Ras-infected cells express relatively high levels of viral Ras proteins, which migrate with a slightly lower mobility than endogenous normal Ras proteins in polyacrylamide gels, as shown by Western immunoblotting with a pan-Ras monoclonal antibody (insert). (c) Erk phosphorylation levels in different cell lines. The relative levels of total and phosphorylated Erk1 and Erk2 proteins were determined as in the legend to Figure 5d. (d) Comparison of Ras activation in PDV cell transfectants. The levels of Ras bound to GTP and Ras protein expression were determined in the cell lysates (0.7 mg of total protein) as in the legend of Figure 4

of Erk at the same extent (90–100%) in all clones (Figure 6a,b). In Ras-infected 3DC and 3DdnS cells, nuclear accumulation of Erk raised maximum levels in basal conditions, masking the effect of TGF-β_1 (Figure 6b). As expected, low levels of phospho-Erk1,2 proteins were found in 3DC and 3DdnS cells. Phosphorylation of both isoforms increased after infection with Ras or stimulation with TGF-β_1 (Figure 6c). In contrast, enhanced levels of phospho-Erk2, but not of phospho-Erk1, were observed in unstimulated PdnS transfectants compared with control PC4 cells (Figure 6c). We also analysed the activity of Ras signalling by comparing the levels of Ras-GTP in PC and PdnS transfectants. PdnS7 and PdnS8 cells showed elevated levels of Ras-GTP respect to control PC4 cells, and this enhancement was not due to increased Ras protein expression (Figure 6d). The same result was obtained with PdnS5 (not shown). These findings are consistent with the idea that inhibition of Smad4 in transformed PDV keratinocytes leads to a constitutive hyperactivation of the Ras/Erk transduction pathway mediated by phosphorylation of Erk2.

Treatment of PDV cells with TGF-β_1 up-regulates uPA expression/secretion associated with stimulation of cell motility and invasiveness (Santibáñez et al., 1999). We show in another report that stimulation of uPA production by TGF-β_1 in PDV cells requires the Ras/Erk signalling pathway (Santibáñez et al., 2000).

Interestingly, PdnS clones consistently secreted increased amounts of uPA compared with control clones (Figure 7a) or the parental cell line (not shown). Treatment with TGF-β_1 for 24 h stimulated uPA production about threefold in PC cells and slightly enhanced the levels of uPA secreted by some PdnS clones (Figure 7a,b). Both basal and TGF-β_1-induced levels of uPA secreted by PdnS cells were inhibited by PD098059 at 50 μM, which also reduced uPA secretion in TGF-β_1-stimulated PC cells, as exemplified with PdnS8 and PC4 clones in Figure 7b. Nevertheless, dominant-negative 3DdnS cells did not increase basal secretion of uPA respect to the parental cell line (Figure 7c) or control clones (not shown). In unstimulated MCA3D cells, secreted uPA was enhanced by overexpression of oncogenic Ras after retroviral infection, and this increase was also inhibited by PD098059 (Figure 7c). The same result was obtained in 3DdnS cells (not shown).

To analyse whether enhanced secretion of uPA in PdnS clones correlated with increased motility, we performed an in vitro wound healing assay comparing the abilities of PC and PdnS clones to repopulate a wound made 24 h before (Figure 8a,b). PdnS clones showed higher migratory abilities than PC in unstimulated conditions. TGF-β_1 enhanced cell motility of all clones, although the effect was more pronounced in control PC cells. To demonstrate the involvement of
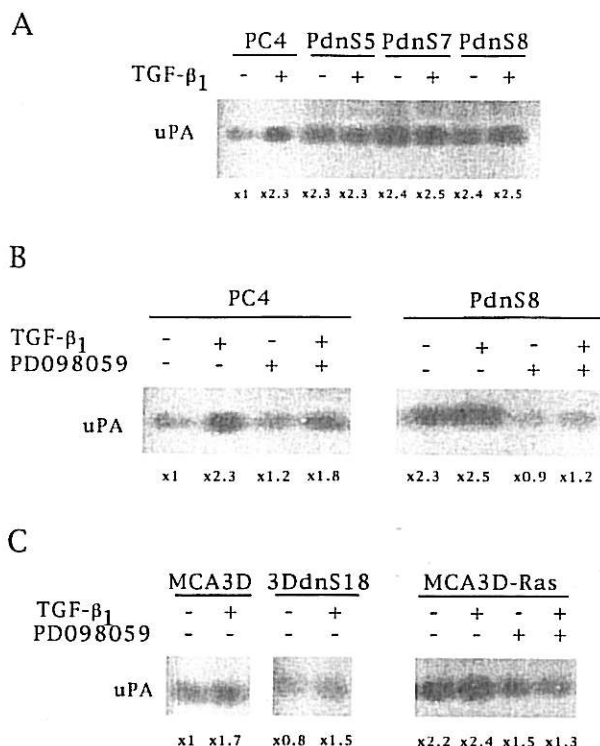
A

PC4 PdnS5 PdnS7 PdnS8

TGF-β_1 - + - + - + - +

uPA

x1 x2.3 x2.3 x2.3 x2.4 x2.5 x2.4 x2.5

B

PC4   PdnS8

TGF-β_1 - + - +   - + - +
PD098059 - - + +   - - + +

uPA

x1 x2.3 x1.2 x1.8   x2.3 x2.5 x0.9 x1.2

C

MCA3D 3DdnS18   MCA3D-Ras

TGF-β_1 - + - +   - + - +
PD098059 - - - -   - - + +

uPA

x1 x1.7 x0.8 x1.5 x2.2 x2.4 x1.5 x1.3

Figure 7 uPA secreted activity is increased in PDV dominant-negative Smad4 cell transfectants. (a) Zymographic analysis of uPA activity determined in the conditioned serum-free media of PDV cell transfectants unstimulated or stimulated with TGF-β_1 for 24 h. (b) Effect of PD098059 (50 μM) on the basal and TGF-β_1-stimulated uPA levels secreted by PDV cell transfectants. (c) uPA activity secreted by non-infected MCA3D and 3DdnS18 cells, and Ras-infected MCA3D cells, unstimulated or stimulated with TGF-β_1 for 24 h. Effect of PD098059. Since MCA3D cells express/secrete 4–5-fold lower levels of uPA than PDV (Santibáñez *et al.*, 1999), aliquots of conditioned media used for determinations of uPA were normalized for a protein concentration of 0.5 μg/μl in (a, b), and of 2.5 μg/μl in (c)

uPA in the motility properties of the cells, we synthesized a peptide (P41–54) comprising aminoacids residues 41–54 of the amino-terminal domain of mouse uPA. This fragment was shown to be a potent antagonist of the binding of uPA to its high affinity cell-surface receptor (Min *et al.*, 1996), and to inhibit TGF-β_1-stimulated cell motility and invasiveness of PDV cells (Santibáñez *et al.*, 1999). As shown in Figure 8a,b, treatment with P41–54 strongly reduced basal cell motility of PdnS cells, and blocked migration stimulated by TGF-β_1 in PC and PdnS clones, while unrelated control peptides had no effect (not shown).

Importantly, a clear change to a fibroblastoid cell morphology was observed in PdnS clones respect to PC or PDV keratinocytes (Figure 8c). 3DdnS transfectants, on the other hand, exhibited morphological appearances (Figure 8c) and low migratory abilities (not shown) similar to that of the parental cell line. To analyse the behaviour of PC and PdnS clones *in vivo*, cells were transplanted into nude mice by i.d. injection and their tumorigenic characteristics compared (Table 1). No significant changes in the rates of tumour growth were observed between PC and PdnS clones, although PC-induced tumours tend to appear earlier. Notwithstanding, a striking difference was observed in the tumour phenotypes (Figure 9, Table 1). PC tumours were histologically typed as well differentiated

squamous cell carcinomas (see PC2 in Figure 9), and only small areas moderately/poorly differentiated were observed in two PC4 tumours (not shown). In PdnS tumours, keratinizing areas were absent (see PdnS8 in Figure 9), or, when present in some tumour sections (two PdnS7 and one PdnS5), representing less than 25% of the total tumour surface. Consequently, all PdnS tumours were typed as poorly differentiated carcinomas.

Discussion

In this study we demonstrate that TGF-β_1 activates both the Ras/MAP kinase and Smad signalling pathways in keratinocytes. Smad signalling mediates TGF-β_1-induced growth arrest and up-regulation of p21^{Cip1} in non-transformed MCA3D keratinocytes, as 3DdnS dominant-negative Smad4 cell transfectants exhibited a block in these responses. In transformed PDV keratinocytes, however, other pathways besides Smad are implicated for TGF-β_1-induced growth inhibition. Modulation of p21^{Cip1} expression by TGF-β_1 in PDV cells is independent of Smad4 and requires Erk MAP kinase signalling activity. Therefore, both the Smad and MAP kinase pathways can be involved in the regulation of p21^{Cip1} expression by TGF-β_1 in keratinocytes. A key factor for the different responses of MCA3D and PDV cells appears to be the presence of an activated Ras gene in the latter cells (Quintanilla *et al.*, 1991). Overexpression of oncogenic Ras in MCA3D cells by retroviral infection induced a high level of p21^{Cip1} protein regardless of blocking Smad4 or not. These levels were comparable to that induced by TGF-β_1 in non-infected cells, and were inhibited by PD098059. The high basal level of p21^{Cip1} observed in Ras-infected MCA3D compared to PDV cells is likely due to the higher oncogenic Ras dosage expressed by 3D-Ras cells. It has been demonstrated that, in certain situations, activation of Ras induces p21^{Cip1} expression and cell cycle arrest via the Erk MAP kinase transduction pathway (reviewed in Lloyd, 1998). Constitutively active Ras requires Rho signalling for suppression of p21^{Cip1} induction (Olson *et al.*, 1998). This mechanism could be operating in PDV cells to maintain low basal levels of p21^{Cip1}. In support of this hypothesis is the observation by Adnane *et al.* (1998) that a dominant-negative mutant of RhoA activates p21^{Cip1} expression, while constitutively active RhoA repress it, in the pancreatic carcinoma cell line Panc-1, which contain an activated K-Ras gene. The fact that TGF-β_1 is able to up-regulate p21^{Cip1} levels in PDV (this study) as well as in Panc-1 cells (Grau *et al.*, 1997) might imply that the growth factor regulates negatively Rho activity. Studies aimed to evaluate the involvement of Rho GTPases in the PDV cell responses to TGF-β_1 are currently in progress.

Nevertheless, the most striking finding in this study is that inactivation of Smad4 in transformed PDV keratinocytes, but not in nontumorigenic MCA3D cells, leads to increased activity of the Ras/Erk signalling pathway; as found by enhanced levels of Ras-GTP, phosphorylated Erk2, and nuclear accumulation of Erk proteins, in dominant-negative PdnS transfectants compared to PC control cells. These observations suggest a new type of interaction by
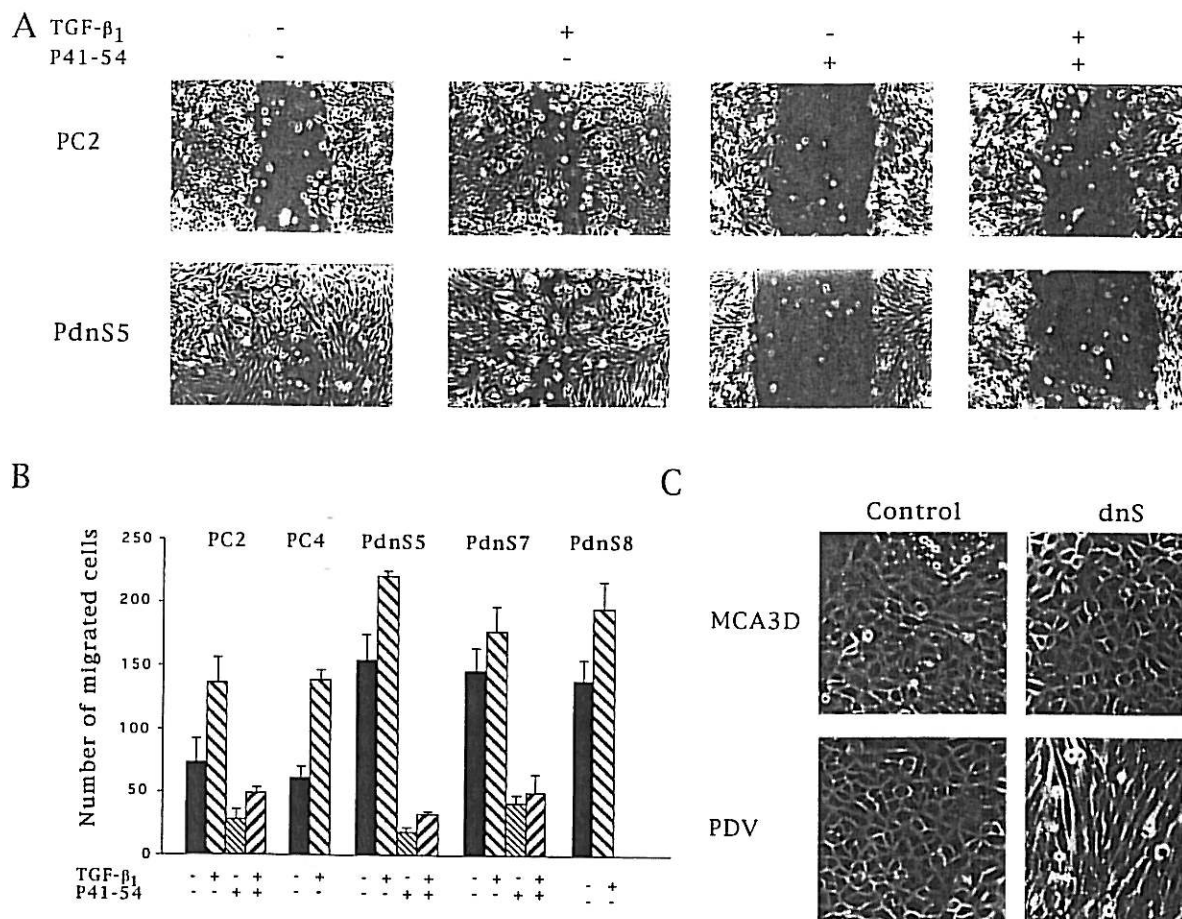
Figure 8 PDV dominant-negative Smad4 cell transfectants exhibit enhanced migratory abilities and a change toward a fibroblastoid cell morphology. (a) Wounds made in subconfluent cell cultures of PC2 and PdnS5 clones were examined after 24 h of culturing in the absence or presence of TGF-β_1. The uPA synthetic peptide P41-45, added at 150 μg/ml, inhibits both basal and TGF-β_1-stimulated cell motility. Bar, 50 μm. (b) Diagram showing quantitation of the cell motility assay made with different PDV cell transfectants. Cells invading the wound were counted in three different fields as those showed in the micrographs. The figure represents the mean values ($\pm$s.d.) of migrated cells in the different experimental conditions. (c) Phase contrast micrographs of representative MCA3D (3DC2, 3DdnS18) and PDV (PC2, PdnS7) cell clones transfected with the neo vector alone or the dominant-negative Smad4 construct. The rest of 3DdnS and PdnS clones exhibited similar morphological appearances as those of 3DdnS18 and PdnS7. Bar, 25 μm

Table 1 Tumorigenicity of the cell lines in nude mice

Cell clone	Tumours/ sites	Latency[a] (weeks)	Tumour histology[b]
PC4	5/5	2.5–4	Well diff. SCC
PC2	6/6	2–3	Well diff. SCC
PdnS5	6/6	4–5	Poorly diff. SCC
PdnS7	5/5	4.5–5	Poorly diff. SCC
PdnS8	5/5	3–5	Poorly diff. SCC

[a]The latency period was estimated as the time needed for tumours to reach a size of 0.5-cm^2. [b]SCC, squamous cell carcinoma

which Smad4, directly or indirectly, inhibits Ras signalling activity in transformed keratinocytes, in addition to the mechanism of repression of Smad signalling by oncogenic Ras/MAP kinases proposed by Kretzschmar et al. (1999). However, the molecular basis for this cross-talk between Smad4 and Ras remains to be investigated.

The functional consequences of inactivating Smad4 in PDV cells are increased secretion of uPA, enhanced motility, and a change toward a fibroblastoid cell morphology associated with the development of poorly differentiated tumours. High levels of secreted uPA are commonly associated with tumoural invasiveness and metastasis and with a poor patient prognosis (Andreasen et al., 1997). The finding that PD098059 reduces uPA secretion in dominant-negative PdnS transfectants to levels similar to that of unstimulated PDV keratinocytes, suggest an involvement of the MAP kinase cascade to regulate enhanced production of uPA in PdnS cells, probably through hyperactivation of Ras signalling activity. In fact, the Ras/MAP kinase pathway is required for TGF-β_1 to modulate uPA expression/secretion in PDV cells (Santibáñez et al., 2000).

Taken together, our results suggest that the presence of an activated Ras gene and loss of Smad4 function cooperates for malignant progression. This co-operation might be physiologically relevant in certain tumours where oncogenic mutations in Ras coincides with functional inactivation of Smad4, as occurs in pancreatic and colon carcinomas. Pancreatic adenocarcinomas exhibit the highest rate of activating Ras (K-Ras) mutations found in human tumours with a frequency above 90% (Almoguera et al., 1988; Rozenblum et al., 1997), and about 50% of carcinomas have inactivated Smad4 (DPC4) (Hahn and Schmiegel,
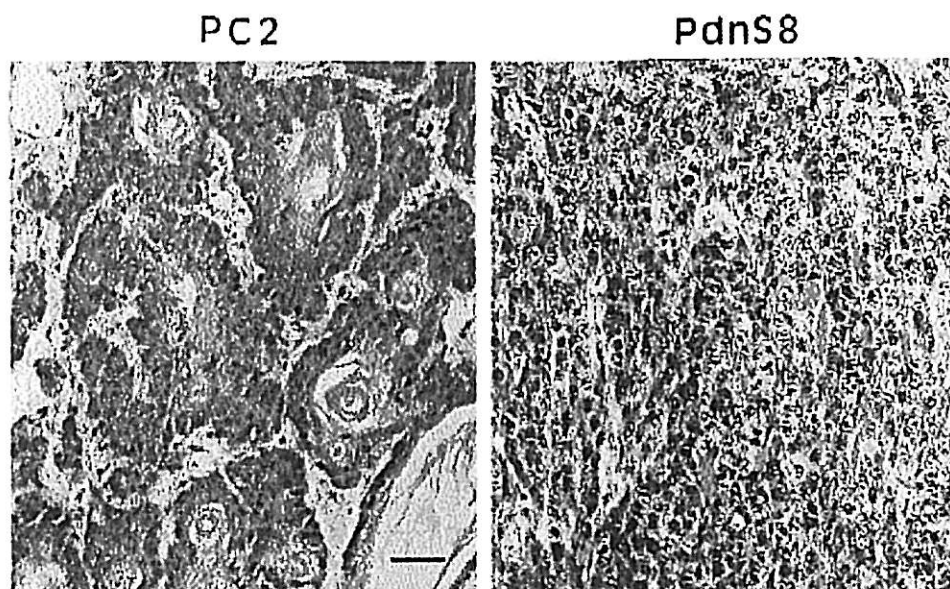
Figure 9 Histological appearance of tumours induced by PDV cell transfectants. PC clones gave rise to well differentiated squamous cell carcinomas as that showed for PC2. PdnS clones produced poorly differentiated tumours as the one showed for PdnS8, in which squamous differentiated components were absent or present only in minority regions. Bar, 30 μm

1998; Rozenblum et al., 1997). These frequencies are lower in colon carcinomas with approximately 50% of the tumours containing mutations in K-Ras (Bos et al., 1987; Burmer et al., 1990) and about 15% loss of Smad4 (DPC4) (MacGrogan et al., 1997; Thiagalingam et al., 1996). It would be of clinical interest to analyse whether the combination of an oncogenic Ras mutation (an early event in carcinogenesis) and inactivated Smad4 suppressor genes (a late event) is a prognostic factor for the development of more malignant undifferentiated carcinomas. In supporting this possibility, a recent study in which more than 100 cell lines and primary tumours were analysed for MAP kinase activity resulted in pancreas and colon tumour cells exhibiting high frequencies of constitutive MAP kinase activation that correlated with a poorly differentiated tumour phenotype (Hoshino et al., 1999). On the other hand, another report has shown that sustained activation of the MAP kinase cascade in MDCK cells leads to an epithelial-fibroblastic conversion associated with increased migratory and invasive properties (Montesano et al., 1999).

Materials and methods

Cell culture, treatment conditions and transfection procedures

The origin and characteristics of MCA3D and PDV cell lines have been described previously in several reports (Quintanilla et al., 1991; Caulín et al., 1995; Santibáñez et al., 1999). Cells were grown in Ham's F-12 medium supplemented with amino acids and vitamins (GIBCO, Ltd., Paisley, Scotland), 10% foetal bovine serum, and antibiotics (2.5 μg/ml amphotericin B, 100 μg/ml ampicillin, and 32 μg/ml gentamicin; Sigma Chemical Co., St. Louis, MO, USA). Cultures were maintained on plastic at 37°C in a 5% CO_2 humidified atmosphere.

MCA3D and PDV cells were co-transfected with an expression vector for the neomycin resistance gene, pcDNA3 (In Vitrogene, San Diego, CA, USA) and plasmids contain-

ing a full-length Smad4/DPC4 cDNA or a C-terminal truncated dominant-negative Smad4/DPC4 (1–514) construct (Lagna et al., 1996), under the control of the cytomegalovirus promoter. The Smad4 plasmids were kindly provided by Dr Joan Massagué (Memorial Sloan-Kettering Cancer Center, New York). Transfections were made in DMEM medium using lipofectamine reagent (Life Technologies, Gaithersburg, MD, USA). Cells were selected in complete Ham's F-12 medium containing 400 μg/ml of G418 (Calbiochem-Novabiochem Co) for 2 weeks, and G418-resistant clones isolated by cloning rings.

Transient co-transfection assays with the 3TP-lux reporter construct and with a lacZ plasmid to score transfection efficiency, were performed as described previously (Santibáñez et al., 1999).

For TGF-β_1 treatments, human recombinant TGF-β_1 (Calbiochem-Novabiochem Intl., La Jolla, CA, USA) was used. The growth factor was added to the cell cultures at a final concentration of 10 ng/ml.

For cell growth assays, cells were synchronized by leaving them at confluence for 24 h. Equivalent numbers of synchronously growing cells were seeded in 20-cm² plates in standard medium. After 18 h, fresh medium with or without TGF-β_1 was added, and the total number of cells determined 48 h later in a Coulter counter.

PD098059 was obtained from Calbiochem-Navabiochem Intl. and added to the cell cultures 20 min prior to stimulation with TGF-β_1, at the indicated concentrations, in serum-free medium. Then, cells were washed and grown in fresh medium, plus or minus serum, in the presence or absence of TGF-β_1.

Infection of MCA3D transfectant clones with the Harvey murine sarcoma virus (carrying the viral H-Ras oncogene) was achieved with high-titer viral supernatants obtained by growing Ψ2-MDRas cells to confluence, as described by Missero et al. (1991).

Wound healing assay

Cellular motility was assayed by an *in vitro* wound model. Subconfluent cell monolayers were gently scratched with a tip to produce a 'wound'. Then, cultures were allowed to grow for 24 h in standard medium with or without TGF-β_1. Synthesis of peptide P41–54 (VSYKYFSRIRRCSC), com-

prising amino acid residues 41–54 of the EGF-like domain of mouse uPA, and unrelated peptides derived from gelatin by limited trypsin degradation, used as a control, are described elsewhere (Santibáñez et al., 1999). Peptides were added to the culture media, at 150 μg/ml, at the same time as TGF-β_1.

Immunofluorescence analysis

Immunofluorescence stainings for Smad2,3 and Erk1,2 proteins were performed by conventional procedures, in cells fixed and permeabilized in cold methanol, with polyclonal antibodies (Santa Cruz Biotechnology Inc., Santa Cruz, CA, USA): E-20, specific for Smad2 and Smad3, and K-23, which recognizes both Erk1 and Erk2 isoforms. Antibodies were used at 1:50 dilution in PBS containing 2% BSA. Rhodamine-conjugated anti-goat and anti-rabbit IgG (Jackson ImmunoResearch Lab., West Grove, PA, USA), respectively, were used as secondary antibodies. Different fields containing 30–60 cells were photographed, and the percentage of cells with Smad2,3 or Erk1,2 accumulated in the nucleus determined counting 10 distinct fields from triplicates corresponding to each experimental situation.

Western blot analysis

Cells were lysed in RIPA buffer (50 mM NaCl, 1% NP-40, 0,5% sodium deoxycholate, 0,1% SDS, 50 mM Tris-HCl, pH 7.5) and a cocktail of proteinase inhibitors (2 μg/ml aprotinin, 2 μg/ml leupeptin and 1 mM phenylmethylsulphonyl fluoride). For phospho-Erk determinations, phosphatase inhibitors: 1 mM sodium orthovanadate, 50 mM sodium fluoride, 10 mM sodium pyrophosphate and 2 mM hydrogen peroxide, were added to the lysis buffer. For Ras protein determinations a lysis buffer containing 100 mM NaCl, 5 mM $CaCl_2$, 5 mM $MgCl_2$, 2% SDS, 50 mM Tris HCl, pH 7.4, and proteinase inhibitors was used. Proteins (20 or 30 μg/lane) were resolved by SDS–PAGE and transferred to Immobilon P membranes (Millipore Corp., Bedford, MA, USA). Ras proteins were detected by a pan-Ras monoclonal antibody (Ab-3, Oncogene Science Inc., Uniondale, NY, USA). For $p21^{Cip1}$ and phospho-Erk1,2 protein determinations, a polyclonal antibody (C-20) and a monoclonal antibody (E-4), respectively, both from Santa Cruz Biothechnology Inc., were used as primary antibodies, followed by exposure to peroxidase-conjugated secondary antibodies (Amersham Intl. Plc. Amersham Bucks, UK), and developed using the enhanced chemoluminescent system (ECL, Amersham Corp., Arlington Heights, FL, USA). The bands detected in the Western blots were quantified by scanning and digitalization of the X-ray films.

Measurement of Ras activation and zymographic assays

The capacity of Ras-GTP to bind the Ras-binding domain of Raf-1 (RBD) was used to analyse the level of active Ras in the cells (de Rooij and Bos, 1997). Briefly, cleared cell lysates (0.7–1.1 mg of total protein) were incubated with 30 μg of the fusion protein GST-RBD bound to glutathione-Sepharose beads. Beads were washed and bound proteins solubilized in Laemmli buffer and resolved in SDS–PAGE. Proteins were then immunoblotted as described above, and precipitated Ras-GTP detected using a pan-Ras monoclonal antibody. The level of Ras protein expression was determined in the cell lysates by Western immunoblotting using the same antibody.

uPA-secreted activity of cell cultures was determined by caseinolytic zymography, as previously reported (Santibáñez et al., 1999). Aliquots (20–30 μl) of conditioned serum-free medium, normalized for the same amount of protein (0.5 μg/μl in PDV experiments, and 2.5 μg/μl in MCA3D experiments), were first subjected to SDS–PAGE under nonreducing conditions, and then to zymography on agarose gels containing casein and plasminogen.

Tumorigenicity assays and histopathology

Suspensions of $1-2 \times 10^6$ cells were injected intradermaly into the flanks of 8–10-week-old Swiss athymic nude mice (CRIFFA, Barcelona, Spain). Animals were observed for tumour formation, and the size of tumours (in cm^2) calculated from caliper measurements of two orthogonal diameters at different times. Histological typing of all developed tumours was performed on formalin-fixed and paraffin-embedded sections by staining with hematoxylin and eosin.

References

Adnane J, Bizouarn FA, Qian Y, Hamilton AD and Sebti SM. (1998). Mol. Cell. Biol., 18, 6962–6970.

Akhurst RJ and Balmain A. (1999). J. Pathol., 187, 82–90.

Alexandrow MG and Moses HL. (1995). Cancer Res., 55, 1452–1457.

Almoguera C, Shibata D, Forrester K, Martin J, Arnheim N and Perucho M. (1988). Cell, 53, 549–554.

Andreasen PA, Kjoller L, Christensen L and Duffy MJ. (1997). Int. J. Cancer, 72, 1–22.

Atfi A, Buisine M, Mazars A and Gespach C. (1997). J. Biol. Chem., 272, 24731–24734.

Bos JL, Fearon ER, Hamilton SR, Verlaan-de Vries M, van Boom JH, van der Eb AJ and Vogelstein B. (1987). Nature, 327, 293–297.

Burmer GC, Levine DS, Kulander BG, Haggitt RC, Rubin CE and Rabinovitch PS. (1990). Gastroenterology, 99, 416–420.

Burns PA, Kemp CJ, Gannon JV, Lane DP, Bremner R and Balmain A. (1991). Oncogene, 6, 2363–2369.

Caulin C, Scholl FG, Frontelo P, Gamallo C and Quintanilla M. (1995). Cell Growth Differ., 6, 1027–1035.

Cui W, Fowlis DJ, Bryson S, Duffie E, Ireland H, Balmain A and Akhurst RJ. (1996). Cell, 86, 531–542.

Datto MD, Li Y, Panus JF, Howe DJ, Xiong Y and Xiao-Fan W. (1995). Proc. Natl. Acad. Sci. USA, 92, 5545–5549.

Davis RJ. (1993). J. Biol. Chem., 268, 14553–14556.

de Rooij J and Bos JL. (1997). Oncogene, 14, 623–625.

de Winter JP, Roelen BAJ, ten Dijke P, van der Burg B and van den Eijnden-van Raaij AJM. (1997). Oncogene, 14, 1891–1899.

Farina AR, Coppa A, Tiberio A, Tacconelli A, Turco A, Colletta G, Gulino A and Mackay AR. (1998). Int. J. Cancer, 75, 721–730.

Frontelo P, González-Garrigues M, Vilaró S, Gamallo C, Fabra A and Quintanilla M. (1998). Exp. Cell Res., 244, 420–432.

Grau AM, Zhang L, Wang W, Ruan S, Evans DB, Abbruzzese JL, Zhang W and Chiao PJ. (1997). *Cancer Res.*, **57**, 3929–3934.

Haddow S, Fowlis DJ, Parkinson K, Akhurst RJ and Balmain A. (1991). *Oncogene*, **6**, 1465–1570.

Hahn SA and Schmiegel WH. (1998). *Digestion*, **59**, 493–501.

Hannon GJ and Beach D. (1994). *Nature*, **371**, 257–261.

Hartsough MT, Frey RS, Zipfel PA, Buard A, Cook SJ, McCormick F and Mulder KM. (1996). *J. Biol. Chem.*, **271**, 22368–22375.

Hartsough MT and Mulder KM. (1997). *Pharmacol. Ther.*, **75**, 21–41.

Hill CS and Treisman R. (1995). *Cell*, **80**, 199–211.

Hoshino R, Chatani Y, Yamori T, Tsuruo T, Oka H, Yoshida O, Shimada Y, Ari-i S, Wada H, Fujimoto J and Kohno M. (1999). *Oncogene*, **18**, 813–822.

Hu PP, Shen X, Huang D, Liu Y, Counter C and Wang X-F. (1999). *J. Biol. Chem.*, **274**, 35381–35387.

Hunt KK, Fleming JB, Abramian A, Zhang L, Evans DB and Chiao PJ. (1998). *Cancer Res.*, **58**, 5656–5661.

Kretzschmar M, Doody J, Timokhina I and Massagué J. (1999). *Genes Dev.*, **13**, 804–816.

Lagna G, Hata A, Hemmati-Brivaniou A and Massagué J. (1996). *Nature*, **383**, 832–836.

Lahio M and Keski-Oja J. (1992). *Crit. Rev. Oncog.*, **3**, 1–26.

Lloyd AC. (1998). *Curr. Opin. Gen. Dev.*, **8**, 43–48.

MacGrogan DL, Pegram M, Slamon D and Bookstein R. (1997). *Oncogene*, **15**, 1111–1114.

Malliri A, Yeudall WA, Nikolic M, Crouch DH, Parkinson EK and Ozanne B. (1996). *Cell Growth Differ.*, **7**, 1291–1304.

Massagué J. (1990). *Annu. Rev. Cell Biol.*, **6**, 597–641.

Massagué J. (1998). *Annu. Rev. Biochem.*, **67**, 753–791.

Min HY, Doyle LV, Vitt CR, Zandonella CL, Stratton-Thomas JR, Shuman MA and Rosenberg S. (1996). *Cancer Res.*, **56**, 2428–2433.

Missero C, Filvaroff E and Dotto GP. (1991). *Proc. Natl. Acad. Sci. USA*, **88**, 3489–3493.

Montesano R, Soriano JV, Hosseini G, Pepper MS and Schramek H. (1999). *Cell Growth Differ.*, **10**, 317–332.

Mucsi I, Skorecki KL and Goldberg HJ. (1996). *J. Biol. Chem.*, **271**, 16567–16572.

Oft M, Heider K-H and Beug H. (1998). *Curr. Biol.*, **8**, 1243–1252.

Oft M, Peli J, Rudaz C, Schwartz H, Beug H and Reichmann E. (1996). *Genes Dev.*, **10**, 2462–2477.

Olson MF, Paterson HF and Marshall CJ. (1998). *Nature*, **394**, 295–299.

Portella G, Cumming SA, Liddell J, Cui W, Ireland H, Akhurst RJ and Balmain A. (1998). *Cell Growth Differ.*, **9**, 393–404.

Quintanilla M, Haddow S, Jonas D, Jaffe D, Bowden GT and Balmain A. (1991). *Carcinogenesis*, **12**, 1875–1881.

Reynisdóttir I, Polyak K, Iavarone A and Massagué J. (1995). *Genes Dev.*, **9**, 1831–1845.

Rozenblum E, Schutte M, Goggins M, Hahn SA, Panzer S, Zahurak M, Goodman SN, Sohn TA, Hruban RH, Yeo CJ and Kern SE. (1997). *Cancer Res.*, **57**, 1731–1734.

Santibáñez JF, Frontelo P, Iglesias M, Martinez J and Quintanilla M. (1999). *J. Cell. Biochem.*, **74**, 61–73.

Santibáñez JF, Iglesias M, Frontelo P, Martinez J and Quintanilla M. (2000). *Biochem. Biophys. Res. Comm.*, **273**, 521–527.

Schwarte-Waldhoff I, Klein S, Blass-Kampmann S, Hintelmann A, Eilert C, Dreschers S, Kalthoff H, Hahn SA and Schmiegel W. (1999). *Oncogene*, **18**, 3152–3158.

Simon C, Juarez J, Nicolson GL and Boyd D. (1996). *Cancer Res.*, **56**, 5369–5374.

Thiagalingam S, Lengauer C, Leach FS, Schutte M, Hahn SA, Overhauser J, Willson JKV, Markowitz S, Hamilton SR, Kern SE, Kinzler KW and Vogelstein B. (1996). *Nature Genetics*, **13**, 343–346.

Yue J, Buard A and Mulder K. (1998). *Oncogene*, **17**, 47–55.

Zhang Y and Derynck R. (1999). *Trends Cell Biol.*, **9**, 274–279.